RAVANA ANGELINI SFALCIN

“AVALIAÇÃO DE PROPRIEDADES FÍSICO-QUÍMICAS DE INFILTRANTES EXPERIMENTAIS COM ADIÇÃO DE PARTÍCULAS DE VIDRO BIOATIVAS”

“EVALUATION OF THE PHYSICAL-CHEMICAL PROPERTIES OF EXPERIMENTAL INFILTRANTS INCORPORATED WITH BIOACTIVE GLASS PARTICLES”

Piracicaba

2015

UNIVERSIDADE ESTADUAL DE CAMPINAS

FACULDADE DE ODONTOLOGIA DE PIRACICABA

RAVANA ANGELINI SFALCIN

"AVALIAÇÃO DE PROPRIEDADES FÍSICO-QUÍMICAS DE INFILTRANTES EXPERIMENTAIS COM ADIÇÃO DE PARTÍCULAS DE VIDRO BIOATIVAS"

"EVALUATION OF THE PHYSICAL-CHEMICAL PROPERTIES OF EXPERIMENTAL INFILTRANTS INCORPORATED WITH BIOACTIVE GLASS PARTICLES"

TESE DE DOUTORADO APRESENTADA À FACULDADE DE ODONTOLOGIA DE PIRACICABA DA UNICAMP PARA OBTENÇÃO DO TÍTULO DE DOUTORA EM MATERIAIS DENTÁRIOS.

DOCTORATE THESIS PRESENTED TO THE PIRACICABA DENTAL SCHOOL OF UNICAMP TO OBTAIN THE Ph.D. GRADE IN DENTAL MATERIALS.

Orientador: Prof. Dr. Americo Bortolazzo Correr

Este exemplar corresponde à versão final de tese defendida por Ravana Angelini Sfalcin e orientada pelo Prof. Dr. Americo Bortolazzo Correr.

Assinatura do Orientador

Piracicaba

2015

Ficha catalográfica
Universidade Estadual de Campinas
Biblioteca da Faculdade de Odontologia de Piracicaba
Marilene Girello - CRB 8/6159

Sfalcin, Ravana Angelini, 1985-
Sf14a Avaliação de propriedades físico-químicas de infiltrantes experimentais com adição de partículas de vidro bioativas / Ravana Angelini Sfalcin. – Piracicaba, SP : [s.n.], 2015.

Orientador: Americo Bortolazzo Correr.
Tese (doutorado) – Universidade Estadual de Campinas, Faculdade de Odontologia de Piracicaba.

1. Microscopia confocal. I. Correr, Americo Bortolazzo,1981-. II. Universidade Estadual de Campinas. Faculdade de Odontologia de Piracicaba. III. Título.

Informações para Biblioteca Digital

Título em outro idioma: Evaluation of the physical-chemical properties of experimental infiltrants incorporated with bioactive glass particles
Palavras-chave em inglês:
Confocal microscopy
Área de concentração: Materiais Dentários
Titulação: Doutora em Materiais Dentários
Banca examinadora:
Americo Bortolazzo Correr [Orientador]
Roberto Ruggiero Braga
Alessandra Bühler Borges
Fernanda Miori Pascon
Simonides Consani
Data de defesa: 27-02-2015
Programa de Pós-Graduação: Materiais Dentários

UNICAMP

UNIVERSIDADE ESTADUAL DE CAMPINAS
Faculdade de Odontologia de Piracicaba

A Comissão Julgadora dos trabalhos de Defesa de Tese de Doutorado, em sessão pública realizada em 27 de Fevereiro de 2015, considerou a candidata RAVANA ANGELINI SFALCIN aprovada.

Prof. Dr. AMÉRICO BORTOLAZZO CORRER

Roberto R Braga

Prof. Dr. ROBERTO RUGGIERO BRAGA

Profa. Dra. ALESSANDRA BÜHLER BORGES

Fernanda Mio Pascon

Profa. Dra. FERNANDA MIORI PASCON

Prof. Dr. SIMONIDES CONSANI

RESUMO

O objetivo neste trabalho foi avaliar as propriedades físico-químicas de infiltrantes resinosos com adição de partículas bioativas, bem como sua capacidade de penetração e dureza da profundidade em lesões subsuperficiais de esmalte. Uma blenda contendo TEGDMA (75% em peso) e BisEMA (25% em peso) foi manipulada e a partir dela foram incorporados 5 tipos de partículas bioativas (10% em peso): hidroxiapatita (HAp), fosfato de cálcio amorfo (ACP), vidro bioativo policarboxilato de zinco (BAG Zn), vidro bioativo 45S5 (BAG 45S5), cimento de silicato de cálcio modificado por β-TCP (HCAT-β). Um material comercial foi utilizado (ICON®) como controle. Dez espécimes foram confeccionados para cada grupo de cada teste: rugosidade superficial (Ra) antes e após a escovação; Resistência à flexão por 3 pontos (RF) e módulo de elasticidade (ME); resistência coesiva à tração (RC); dureza Knoop (KHN); densidade de ligação cruzada (DLC); grau de conversão (GC); sorção (S) e solubilidade (SL) em água; e micro-dureza (KHN). Os dados foram submetidos a ANOVA e teste Tukey (α=0.05). A penetração dos infiltrantes resinosos no esmalte humano desmineralizado foi qualitativamente avaliada em Microscopia Confocal de Varredura a Laser (n=5). Os resultados mostraram que os menores valores de rugosidade (antes e após a escovação foram apresentados pelo ACP. Com relação à resistência a flexão e módulo de elasticidade, T+B apresentou o maior valor e ICON® mostrou o menor valor. ICON® também mostrou o menor valor de resistência coesiva à tração; não houve diferença significativa entre os grupos T+B, HAp, ACP, BAG Zn, BAG 45S5 e HCAT-β. Para o teste de dureza Knoop, ICON® obteve o menor valor e BAG Zn mostrou o maior valor. Para densidade de ligação cruzada, ICON® apresentou maior quantidade de ligação cruzada e HAp, menor quantidade de ligação cruzada. ICON® apresentou grau de conversão significantemente menor que os infiltrantes experimentais, que não diferiram entre eles. ICON® apresentou a maior sorção de água e HAp a menor. Não houve diferença significativa entre os demais grupos. Para solubilidade, ICON® apresentou os maiores valores, mas sem diferença de ACP. BAG 45S5 apresentou a menor solubilidade. Com relação a micro-dureza, não houve diferença estatisticamente significante entre as profundidades avaliadas (50 µm, 200 µm, 350 µm e 500 µm). BAG 45S5, BAG Zn e HCAT-β não mostraram diferença estatística entre eles. Entretanto, HCAT-β e BAG Zn foram similares ao ICON® e ACP. O grupo cariado mostrou menor valor quando comparado a todos os grupos testados. A análise em microscopia confocal mostrou que todos os materiais apresentaram boa capacidade de penetração nas lesões iniciais, exceto para FCA. Pôde ser concluído que adição de partículas bioativas em um infiltrante experimental melhorou as propriedades mecânicas e não afetou a capacidade de penetração dos infiltrantes. O infiltrante resinoso contendo fosfato de cálcio amorfo foi o que apresentou o melhor desempenho no teste de rugosidade de superfície antes e após a escovação.

Palavras-chave: Microscopia Confocal, remineralização dentária, propriedades físicas, propriedades químicas, resinas

ABSTRACT

The aim of this study was to evaluate the physical-chemical properties of the experimental infiltrants with the addition of bioactive particles as well as their capability of penetration and depth Knoop hardness into caries-like lesions. A control blend was made with TEGDMA (75 wt%) and BisEMA (25 wt%). Five bioactive fillers were added in the control blend (10 wt%): Hydroxyapatite (Hap), amorphous calcium phosphate (ACP), Zinc-polycarboxylated bioactive glass (BAG-Zn), bioactive glass 45S5 (BAG 45S5), and β-TCP modified calcium silicate cements (HCAT-β). An available commercially material was used (ICON®). Ten specimens were comprised by each group for the following tests: Surface roughness (Ra) before and after brushing abrasion; flexural strength (FS) and elastic modulus (*E*-Modulus); tensile cohesive strength (TCS); Knoop hardness (KHN); softnening ratio (SR); degree of conversion (DC); water sorption (WS) and solubility (SL); and micro-hardness (micro-KHN). Data were subjected to ANOVA and Tukey's test ($\alpha=0.05$). Confocal Scanning Laser Microscopy was used to evaluate qualitatively the penetration capability of resin infiltrants into demineralized human enamel. Results showed that ACP had the lowest Ra before and after brushing abrasion. Regarding to the FS and *E*-modulus, T+B showed the higher value and ICON® showed the lower value. Also, ICON® showed the lower value of TCS, but there was no significant statistically difference among the groups T+B, HAp, ACP, BAG Zn, BAG 45S5 e HCAT-β. To the KHN, ICON® obtained the lower value and BAG Zn showed the higher value. According to the SR, ICON® showed lower SR and HAp, the higher SR. ICON showed DC significantly lower than experimental resin infiltrants. Regarding to the WS, ICON® presented the highest water sorption and HAp the lowest one. There was no significant statistically difference among the other groups. ICON showed the highest SL results; however, the results were similar to ACP. The lowest SL was found for BAG 45S5. Regarding to the micro-KHN, there was no statistically difference among the analyzed depths (50 µm, 200 µm, 350 µm and 500 µm). BAG 45S5, BAG Zn and HCAT- β did not show statistical difference among them. However, HCAT- β and BAG Zn were similar to ICON® and ACP. Carious group showed lower value when compared to all the tested groups. Confocal microscopy analysis showed good capability of penetration into the initial lesions for all materials, except for ACP. It could be concluded that the addition of bioactive particles into an experimental infiltrant improved the mechanical properties and did not affect the capability of penetration into the experimental infiltrants. The resin infiltrant with amorphous calcium phosphate presented the best performance to the roughness surface before and after brushing abrasion.

Key-words: confocal microscopy, tooth remineralization, physical properties, chemical properties, resins

SUMÁRIO

DEDICATÓRIA

A **Deus**, que sempre me deu forças para seguir meu caminho, me guiando e me protegendo por todos esses anos, e que hoje me concede mais essa conquista.

Aos meus pais, **Jorge e Márcia**, por todo amor, compreensão, paciência e companheirismo em todos estes anos.

Aos meus irmãos **Renato e Roberta**, por todo amor e carinho, pelo apoio e força que sempre me deram para que eu alcançasse todos os meus objetivos.

À minha sobrinha **Vitória**, por ser um anjinho na minha vida, me dando forças para continuar, principalmente no período do meu doutorado-sanduíche.

Ao meu namorado **Márcio**, por todo amor e paciência, principalmente na reta final do doutorado.

AGRADECIMENTOS

À Direção da Faculdade de Odontologia de Piracicaba, da Universidade Estadual de Campinas, na pessoa do seu Diretor **Guilherme Elias Pessanha Henriques**.

Ao meu orientador **Prof. Dr. Américo Bortolazzo Correr** pelos ensinamentos, apoio e atenção concedidos durante todos esses anos do meu doutorado.

Aos **Profs. Drs. Mário Alexandre Coelho Sinhoreti, Mario Fernando de Goes, Simonides Consani e Lourenço Correr Sobrinho**, titulares da área de Materiais Dentários, à **Prof^{a}. Dr^{a}. Regina Maria Puppin-Rontani**, da área de Odontopediatria, ao **Prof. Dr. Marcelo Giannini**, da área de Dentística, e a todos os outros professores do curso de Pós-Graduação em Materiais Dentários pelos ensinamentos, pelo respeito e exemplos dados durante todo o período do doutorado.

Ao meu orientador em Londres **Prof. Timothy Frederick Watson** e meu co-orientador **Prof. Salvatore Sauro** pela aprendizagem e pela oportunidade oferecida para o meu estágio no exterior. Também aos técnicos do laboratório **Richard Mallet** e **Peter Pilecki** e ao **Dr. Giuseppe Cama** pela amizade e auxílio nas várias metodologias que aprendi. Agradeço também todo o apoio, paciência e auxílio da secretária **Karamjit Rayit.**

Ao **Prof. Guy Carpenter**, por ter me cedido o uso do Microscópio Confocal no King's College, em Londres, e me orientado com relação as recomendações.

Aos técnicos da Área de Materiais Dentários, **Marcos Blanco Cangiani** e **Selma Aparecida Barbosa de Souza Segalla**, pelo auxílio em todos os momentos e pelas horas de amizade e aprendizado durante o período do doutorado.

Ao mestre e amigo **Adriano Luís Martins** e amiga **Eliene Aparecida Orsini Narvaes**, técnicos de microscopia eletrônica da FOP-UNICAMP, com quem aprendi muito sobre microscopia.

Ao técnico **Marcelo Maístro,** do laboratório de Odontopediatria, por toda paciência, auxílio e ensinamentos concedidos durante o Mestrado e o Doutorado.

Aos tantos amigos do Mestrado e do Doutorado e de outras turmas e cursos de Pós-Graduação; **Cesar Pomacóndor, Gabriel Albuná, Rafael Vitti, Ariene Leme, Ailla Lancelloti, João Paulo Silva, Lucas Dantas, Luís Raposo, Garrit Koller, Ashvin Babbar, Shathani Nkhwa, Bernardine Idowu, Pedro Henrique Freitas, Valéria Bisinoto, Ana Paula Ayres, Fabián Murillo, Renata Lacerda, Thales Cândido, Raquel Rodrigues, Eveline Soares, Guilherme Bottene, Polliane Carvalho, Carlos da Cunha Oliveira Júnior**.

Às minhas amigas, parceiras e companheiras **Tatiany Gabrielle Freire Araújo, Roberta Galleti, Isadora Rabelo Guimarães e Ana Paula Piovezan Fugolin,** por tantos momentos de vitórias e obstáculos divididos por todos esses anos.

À minha amiga **Klíssia Romero Felizardo**, por todo companheirismo durante o doutorado sanduíche, pelos momentos bons e difíceis compartilhados e por toda a paciência e compreensão.

A todos os meus familiares e amigos pelo apoio e incentivo compartilhado sempre.

A todos que participaram e torceram direta ou indiretamente desta etapa da minha vida, contribuindo para a conclusão deste curso.

Por fim, um agradecimento especial ao meu amigo **Prof. Dr. Victor Pinheiro Feitosa,** que foi essencial no desenvolvimento da minha pesquisa e pela amizade por todos esses anos.

Meus sinceros agradecimentos!

EPÍGRAFE

“Quanto mais me aprofundo na Ciência, mais me aproximo de Deus”

(Albert Einstein)

INTRODUÇÃO

O desenvolvimento da cárie é um processo dinâmico envolvendo períodos de desmineralização e remineralização (Silverstone, 1977). A cárie dental é uma doença multifatorial que resulta de um desequilíbrio entre fatores patológicos e protetores. Bactérias cariogênicas, carboidratos fermentáveis e disfunção salivar são cientificamente aceitos como importantes fatores patológicos. O desequilíbrio produzido irá resultar em uma ruptura do processo fisiológico de remineralização e desmineralização da estrutura dental, favorecendo o último (Featherstone, 2006). Durante o desenvolvimento de lesões de cárie subsuperficiais em esmalte, o mineral é removido do esmalte, resultando em aumento das porosidades do esmalte, que aparecem clinicamente como as chamadas 'lesões de mancha branca' (Ten Cate *et al.*, 2003).

Alguns estudos (Reynolds, 2008a; Reynolds *et al.*, 2008b; Rao e Malhotra, 2011; Reynolds *et al.*, 2009; Walker *et al.*, 2010; Banerjee *et al.*, 2011) têm sido realizados a fim de desenvolver técnicas de intervenção mínimas para o tratamento de lesões de cárie, ou seja, avaliar as possíveis opções de tratamento menos invasivo a fim de diminuir a perda de tecido e o desconforto do paciente (Rao e Malhotra, 2011). O princípio básico da intervenção mínima é tentar a remineralização de lesões iniciais em substituição à técnica invasiva tradicional para lesões superficiais não cavitadas em esmalte (Rao e Malhotra, 2011). Simplificadamente, a remineralização pode ser descrita como um ganho de mineral em esmalte previamente desmineralizado, seguindo eventos sucessivos de desmineralização e remineralização, mais resistente a subsequentes desafios ácidos do que o mineral original (Lynch e Smith, 2012).

Os tratamentos não invasivos mais comumente utilizados nas lesões de cárie em esmalte não cavitadas incluem a aplicação tópica de flúor, a orientação quanto à higiene oral e os hábitos alimentares dos pacientes. Entretanto, esses métodos apresentam algumas limitações em pacientes não colaboradores, assim como em lesões proximais cavitadas e fóssulas e fissuras de superfícies oclusais (Kidd e Van Amerongen, 2003). A aplicação tópica de flúor tem sido empregada a fim de remineralizar a lesão inicial de cárie; porém, análises clínicas (Bjarnason e Finnbogason, 1991) e dados já estabelecidos sugerem que este método é mais efetivo em prevenir o estabelecimento de lesões iniciais do que sua progressão. A paralisação ou reversão da lesão, devido à desmineralização, é importante em termos de mecanismo de ação do flúor, mas o flúor é mais efetivo na superfície da lesão de cárie. Isso pode levar a uma remineralização na zona superficial não alcançando o corpo da lesão, tornando a completa remineralização difícil de ser alcançada (ten Cate e Arends, 1980).

O uso de materiais infiltrantes nas lesões iniciais de cárie em esmalte tem sido utilizado como uma técnica alternativa (Meyer-Lueckel e Paris, 2008). Ao contrário do selamento convencional de cárie, onde a camada de resina é criada na superfície do esmalte, o uso de materiais infiltrantes nas lesões de cárie subsuperficiais em esmalte tem como objetivo penetrar o corpo da lesão porosa com resinas de baixa viscosidade, as quais são subsequentemente polimerizadas (Paris *et al.*, 2007a; Meyer Lueckel e Paris, 2008a). Uma vez que as porosidades de cárie em esmalte agem como caminhos de difusão para ácidos e minerais dissolvidos, a infiltração destas lesões com resinas pode ocluir estes caminhos, levando à paralisação da progressão da lesão de cárie (Paris *et al.*, 2007a). Entretanto, esta técnica possui algumas limitações, como radiolucidez da lesão infiltrada, o que dificulta a análise do quanto o infiltrante penetrou e o sucesso do tratamento após a infiltração, e incapacidade dos infiltrantes de remineralizar o esmalte adjacente.

A remineralização de lesões subsuperficiais em esmalte tem sido alcançada por soluções de fosfato de cálcio estabilizado por fosfopeptídeo de caseína (Reynolds *et al.*, 2003; Reynolds *et al.*, 2008) e um selante polimérico de fosfato de cálcio amorfo (ACP) (Skrtic *et al.*, 1996). Compósitos contendo partículas de fosfato de cálcio são promissores para combater a cárie. Estes compósitos têm mostrado liberar íons Ca e P e remineralizar as lesões do dente *in vitro* (Dickens *et al.*, 2003; Langhorst *et al.*, 2009).

O vidro bioativo é um biomaterial que tem sido amplamente estudado no campo da engenharia de tecidos, regeneração óssea e remineralização dentinária devido a sua capacidade bioativa notável em formar apatita hidroxicarbonatada (HCA) quando submersa em simulações de soluções fluidas (Vollenweider *et al.*, 2007; Ana *et al.*, 2003;). O biovidro 45S5 (fosfossilicato de sódio e cálcio bioativo – BAG 45S5) é atualmente usado na Odontologia em procedimentos de ”air-cutting”, que sugere um preparo de cavidade minimamente invasivo e como dessensibilizante dentinário (Banerjee *et al.*, 2010). Além disso, o biovidro 45S5 é um dos principais materiais bioativos com excelente habilidade em induzir a precipitação de fosfato de cálcio (Ca/P) e subsequente cristalização na hidroxiapatita quando imerso em solução fluida simulada livre de proteína ou saliva (Sauro *et al.,* 2012).

A partir desta tecnologia, outras formulações de biovidros têm sido estudadas no intuito de melhorar a capacidade de remineralização dos tecidos dentários, como a incorporação de zinco (Zn) na formulação do biovidro (Wang *et al.*, 2006; Lusvardi *et al.*, 2008). Tem sido demonstrado que a liberação de pequena concentração de Zn incorporado a um material implante pode promover a formação de osso ao redor desse implante e acelerar a recuperação dos pacientes (Ito *et al.*, 2000; Ito, *et al.*, 2002; Yamaguchi *et al.*, 1986). O Zn é bem conhecido por suas propriedades antimicrobianas e é componente do adesivo dental como um agente de ligações cruzadas que promove a adesão (Söderholm, *et al.*, 2003). Estudos com biovidro têm sido realizados em dentina, porém, em esmalte, não há relatos sobre o desempenho destes materiais.

Além disso, outro fator importante a ser estudado é a resistência (física, química e mecânica) dos materiais no meio oral tanto quanto suas características de manipulação nos procedimentos restauradores. Diferentes técnicas de ensaios mecânicos tem sido estudados para vários tipos de resistência de compósitos fluidos (Sumino *et al.,* 2013; Bonilla *et al.,* 2003; St-Georges *et al.,*2003). A resistência pode ser definida como a tensão máxima requerida para fraturar uma estrutura ou material. É chamado resistência a flexão, resistência compressiva, ou resistência à tração diametral dependendo do tipo de tensão predominante presente (Hirayama *et al.,* 2014). O grau de conversão das resinas é o principal fator que influencia nas propriedades físicas dos materiais. Em geral, quanto maior a conversão das duplas ligações, maior a resistência mecânica dos materiais (Sideridou *et al.,* 2002). Embora o grau de conversão seja um fator importante, ele não fornece uma completa caracterização da estrutura polimérica, uma vez que os polímeros com grau de conversão similares podem exibir diferentes densidades de ligação cruzadas devido às diferenças na reticulação das cadeias (Asmussen e Peutzfeldt, 2001; Schneider *et al.*, 2008). A densidade de ligação cruzada pode ser indiretamente avaliada medindo o amolecimento dos polímeros durante sua exposição ao etanol (Guiraldo *et al.,* 2009; Schneider *et al*., 2008). O teste de amolecimento é baseado em medidas de dureza repetidas antes e após a imersão das amostras em solventes orgânicos (Schneider *et al*., 2008).

Idealmente, as redes poliméricas deveriam ser materiais insolúveis com estabilidade química e térmica relativamente altas. Entretanto, a maioria dos monômeros utilizados nos materiais resinosos podem absorver água e elementos químicos do meio, e também liberar componentes para o meio circundante (Santerre *et al.*, 2001; Ferracane, 2004). Dessa forma, a sorção de água e solubilidade levariam a uma variedade dos processos químicos e físicos que podem resultar em efeitos deletérios na estrutura e função de polímeros dentais, incluindo sua capacidade retentiva em adesivos, por exemplo (Malacarne *et al*., 2006).

Testes de rugosidade superficial e desgaste após a simulação de escovação também tem sido indicados a fim de avaliar os materiais restauradores (Cilli *et al.*, 2009; Prakki *et al.*, 2008). Mesmo que o processo de escovação tenha um papel importante na higiene oral, sua ação contínua pode danificar a superfície das restaurações, tornando-a mais rugosa e, conseqüentemente, mais propícias ao manchamento, ao acúmulo de placa, a inflamação do tecido mole e cáries recorrentes (Garcia *et al.*, 2004; Yap *et al*., 2005).

Além dos testes mecânicos utilizados para avaliar as propriedades dos materiais utilizados na Odontologia, outras análises são necessárias para avaliar o comportamento dos materiais no substrato estudado. Pesquisadores tem utilizado um número considerável de técnicas analíticas a fim de quantificar e qualificar as mudanças ocorridas no conteúdo mineral de esmalte durante a formação da lesão de cárie (Lippert e Lynch, 2014). A maioria das técnicas frequentemente empregadas são a micro radiografia transversal (Bergman e Engfeldt, 1954), microdureza Knoop (Sweeney, 1942) e Vickers (Gustafson e Kling, 1948) inicialmente usadas de forma perpendicular ou paralelas (Davidson *et al.,* 1974) à superfície do tecido duro, microscopia de luz polarizada (Carlström, 1964) e microscopia confocal de varredura a laser (Jones e Boyde, 1987).

Diante de todos esses fatores, é de suma importância avaliar as propriedades mecânicas, físicas e químicas dos materiais assim como sua capacidade de penetrar nas lesões iniciais de cárie em esmalte, e reforçar a estrutura perdida de esmalte. Dessa forma, a incorporação de partículas bioativas na composição de infiltrantes resinosos poderia ser uma boa alternativa para reforçar as lesões subsuperficiais de cárie em esmalte assim como paralisar a progressão destas lesões e evitar a desmineralização dos tecidos dentais adjacentes à lesão de cárie. Portanto, o objetivo neste estudo foi avaliar as propriedades físico-químicas de infiltrantes resinosos com adição de partículas bioativas, bem como sua capacidade de penetração e reforço da estrutura perdida em lesões subsuperficiais de esmalte. Estudos futuros serão realizados para avaliar a capacidade de remineralização das partículas bioativas utilizadas neste trabalho.

CAPÍTULO 1

Chemical-mechanical properties of experimental resin infiltrants incorporated with bioactive particles.

ABSTRACT

Objective: The aim of this study was to evaluate the effect of addition of bioactive particles on chemical-mechanical properties of resin infiltrants. .

Methods: Groups were set up as follows: T+B (TEGDMA 75 wt% + BisEMA 25 wt%); HAp (T+B+ Hydroxyapatite 10 wt%); ACP (T+B+ amorphous calcium phosphate 10 wt %); BAG Zn (T+B+ bioactive glass Zn 10 wt%); BAG 45S5 (T+B+ bioactive glass 45S5 10 wt%); HCAT-β (T+B+ β-TCP modified calcium silicate cements 10 wt%) and ICON®. Specimens were comprised by each group for the following tests: degree of conversion (DC) (n=3), Knoop Hardness Number (KHN) (n=10), cross-link density (CLD) (n=10), tensile cohesive strength (TCS) (n=10), flexural strength (FS) (n=10) and Elastic Modulus (*E*-Modulus) (n=10). To water sorption (WS) and solubility (SL) analysis, thirty five specimen disks (n=5) were prepared by dispensing the uncured resin into a mould (6.0 mm x 1.0 mm). After desiccation, the cured specimens were weighed and then stored in distilled water for evaluation of the water diffusion kinetics over 7 days at 37ºC. Data were subjected to one-way ANOVA and Tukey's test (p=5%).

Results: For DC, HCAT-β and ACP showed the highest values and ICON® showed the lowest value. To KHN outcomes, HAp, ACP, BAG Zn and HACT-β were statistically similar among them, however, BAG Zn presented the highest value, and ICON®, the lowest. SR of the infiltrants showed no statistical differences among the experimental infiltrants containing bioactive particles (HAp, ACP, BAG Zn, BAG 45S5 and HCAT-β). BAG 45S5 showed the highest value and ICON® showed the lowest. TCS was statistically similar for all the experimental materials; however, T+B showed the highest value and ICON® still presented the lowest value. For FS, T+B presented the highest value, however, ICON® showed the lowest. *E*-Modulus was statistically similar for all experimental materials incorporated with bioactive particles. Regarding to the WS, ICON® did not show significant statistically difference when compared to ACP and BAG 45S5; however, it showed the highest value of WS, and HAp showed the lowest. SL results showed that ICON® was statistically similar to ACP, and both presented the highest values. Otherwise, BAG 45S5 showed the lowest value, and it was not statistically different of BAG Zn, HCAT-β, HAp and T+B.

Conclusion: the resin infiltrants presented better performance regarding the chemical-mechanical properties than the commercial infiltrant ICON®. The addition of bioactive particles in the experimental materials improved the chemical and mechanical properties.

Key-words: tensile strength, hardness, hydroxyapatite,

1. INTRODUCTION

Treatment of caries requires the understanding that caries development is a dynamic process involving periods of demineralization and remineralization (Silvertsone, 1977). Dental caries is a multifactorial disease that results from an imbalance between pathological and protective factors. Cariogenic bacteria, fermentable carbohydrates, and salivary dysfunction are scientifically accepted as important pathological factors. The imbalance produced will result in a rupture of the physiological processes of remineralization and demineralization of the dental structure, favoring the latter (Featherstone, 2006). Teeth are constantly going through cycles of mineral loss (oral pH is below or at the point at which tooth mineral begins to dissolve) and repair (conditions favor the redeposition of mineral). The net loss or gain in mineral over time determines whether tooth decay will advance, stabilize or regress. The ultimate goal of clinical intervention is the preservation of tooth structure and the prevention of lesion progression to the point where restoration is required (Langhorst *et al.*, 2009).

During the development of subsurface caries lesions, minerals are dissolved out of the enamel, resulting in increased porosities that appear clinically as so-called “white spot” lesions (ten Cate *et al.*, 2003). Such lesions result from the dissolution of calcium hydroxyl apatite from the enamel and the production of microporosities within the remaining calcified tissue (Robinson *et al.*, 1995). These lesions are commonly treated by enhancing remineralization, e.g., through improved oral hygiene, fluoridation (Paris *et al.*, 2007). Remineralization might be described as the delivery of calcium and phosphate, from outside the tooth, into the enamel lesion, effecting deposition of mineral onto the demineralized enamel within (Lynch and Smith, 2012).

The efficacy of caries infiltration in reducing caries progression has been reported in clinical studies (Ekstrand *et al.*, 2010; Paris *et al.*, 2010; Martignon *et al.*, 2012; Meyer-Lueckel *et al.*, 2012). Caries infiltration aims to occlude the pathways since porosities of enamel caries act as diffusion pathways for acids and dissolved minerals, and thus, leading to an arrest of caries progression (Paris *et al.*, 2007). In this way, there are no studies which report the infiltration of the materials using bioactive particles in order to remineralize the demineralized enamel besides to hamper its lesion progression.

Furthermore, it is also relevant to study the mechanical properties of the dental materials such as the strength (physical, chemical and mechanical) of composites in the oral environment as well as the handling characteristics of the materials in restorative procedures (Hirayama *et al.*, 2014). Various strengths of flowable composites have been evaluated by different mechanical testing techniques (Sumino *et al.,* 2013; Bonilla *et al.,* 2003; St-Georges *et al.,* 2003). Strength is the maximum stress required to fracture a structure or material. Depending on the predominant type of stress present, it can be called flexural strength, compressive strength or diametral tensile strength (Hirayama *et al.*, 2014). The material strength can be correlated to its degree of conversion as the degree of conversion of resins is a major factor influencing their physical properties (Sideridou *et al.*, 2002). The higher the degree of conversion, the better the surface properties such as hardness, elastic modulus, resistance to fracture and diametral tensile strength. However, the abovementioned mechanical properties depend on the type of polymeric chain and cross-link density formed during the polymerization process (Yap *et al.*, 2004). Although degree of conversion is an important factor, it does not provide a complete characterization of the network structure, as polymers with similar degree of conversion might exhibit different cross-link densities because of differences in chain linearity (Asmussen and Peutzfeldt, 2001; Schneider *et al.*, 2008). Previous studies showed that cross-link density may be indirectly assessed by measuring the softening of polymers during exposure to ethanol (Guiraldo *et al.,* 2009; Asmussen and Peutzfeldt, 2001). Also, conversion is related to decreased sorption of fluids and solubility of resin composites in the oral environment, which is crucial for a long-lasting clinical performance (Sideridou, 2003). Chemical degradation is usually caused by oxidation and hydrolysis, which are processes that require the presence of water (Ferracane, 2006).

In this manner, this study aimed to add different types of bioactive particles into an experimental infiltrant material in order to evaluate their mechanical properties such as degree of conversion, Knoop hardness, cross-link density, tensile cohesive strength, flexural strength and Elastic Modulus as well as the water sorption and solubility and compare to an available commercially infiltrant. The hypothesis tested was that the experimental infiltrants (with or without the addition of bioactive particles) would present better chemical and mechanical properties when compared to an available commercially infiltrant.

2. MATERIALS AND METHODS

2.1. Experimental infiltrant preparation

The compositions of resin infiltrants are described in **Table 1**. Monomers triethyleneglycol dimethacrylate (TEGDMA – 75 wt%) (Sigma-Aldrich Inc., St. Louis, MO, USA, Batch #01612M) and ethoxylated bisphenol A glycidyl dimethacrylate (BisEMA – 25 wt%) (Sigma-Aldrich Inc., St. Louis, MO, USA, Batch #03514HF) were used as an experimental control blend. Hydroxyapatite (Sigma-Aldrich Inc., St. Louis, MO, USA), amorphous calcium phosphate (Sigma-Aldrich Inc., St. Louis, MO, USA), bioactive glasses particles (BAG-Zn, BAG 45S5) and β-tricalcium phosphate modified calcium silicate cements (HCAT-β) bioactive particles were added in each control blend (10 wt%). After that, the experimental infiltrant materials were left to agitate for 24 h, and also, before the application on the enamel lesion, the materials were slightly agitated again. The photoinitiatior system selected was camphorquinone (CQ) (Sigma-Aldrich Inc., St. Louis, MO, USA, Batch #532604), and dimethyl aminoethyl methacrylate (DMAEMA) (Sigma-Aldrich, Inc., St.

Louis, MO, USA, Batch #BCBF8391V) (proportion 1:2 by weight; 0.5% CQ/1% DMAEMA).

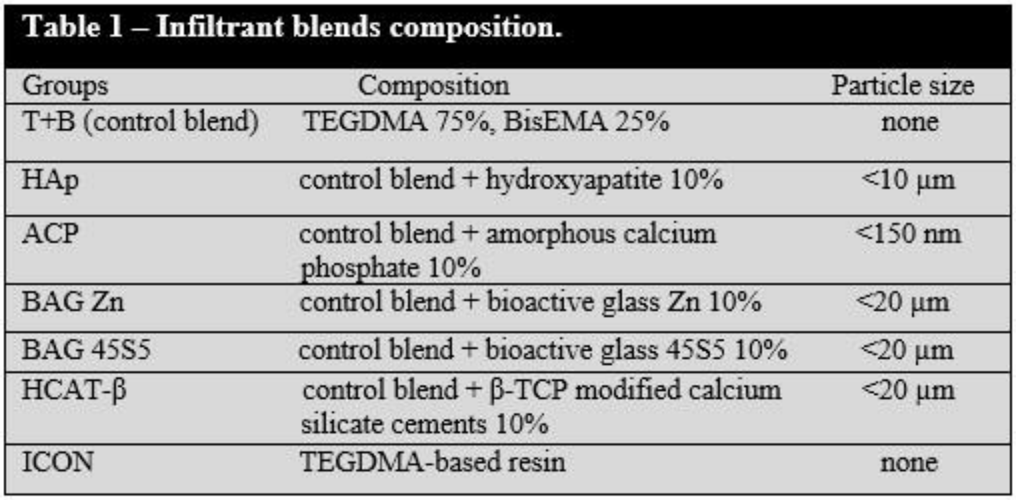

Table 1 – Infiltrant blends composition.

Groups	Composition	Particle size
T+B (control blend)	TEGDMA 75%, BisEMA 25%	none
HAp	control blend + hydroxyapatite 10%	<10 µm
ACP	control blend + amorphous calcium phosphate 10%	<150 nm
BAG Zn	control blend + bioactive glass Zn 10%	<20 µm
BAG 45S5	control blend + bioactive glass 45S5 10%	<20 µm
HCAT-β	control blend + β-TCP modified calcium silicate cements 10%	<20 µm
ICON	TEGDMA-based resin	none

% (wt%); TEGDMA: triethylene glycol dimethacrylate; BisEMA: ethoxylated bisphenol-A dimethacylate.

2.2. Degree of conversion (DC)

The resin infiltrant was dropped on the base of FTIR (n=3) and heights of peaks were collected according to the aliphatic and aromatic peaks. Immediately after that, the same drops were light-cured for 40 s and new heights of peaks were collected. Degree of conversion (DC) was measured by Fourier Transform Infrared Spectroscopy (FTIR-Spectrum One, Perkin Elmer Ltd., Beaconsfield, UK). DC was determined from the aliphatic C=C and aromatic C=C peaks for unpolymerized and polymerized resin, according to a previous standard baseline technique (Rueggeberg *et al.*, 1990). The remaining uncoverted double bonds were determined by comparing the ratio of the aliphatic C=C absorption peak at 1638 cm^{-1} to the carbonyl group C=O peak at 1716 cm^{-1} between the polymerized and unpolymerized specimens (Atai *et al.*, 2004). The absorption of the carbonyl C=O stretching band performed as an internal standard, because it remains constant during the polymerization reaction. The monomer conversion was determined by subtracting the percentage of residual aliphatic C=C bonds from 100%.

2.3. Knoop Hardness Number (KHN) and Softening ratio (SR)

Seventy square shaped specimens (5 mm width x 5 mm length x 2 mm thickness) were made using a polyvinylsiloxane mould (Aquasil LV, Dentsply DeTrey, Denver, USA). The materials were inserted into each mould and the upper surface was covered with a polyester strip (Mylar strip, Keystone Ind. GmbH, Singen, Germany) and pressed with a glass slide to squeeze out any excess of material before the light-curing procedures. The specimens (n=10) were light-cured at 600 mW/cm^2 for 60 s (Optilux VLC; Demetron, CT, USA), and removed from the moulds. After storage for 24 hours (dry storage), the specimens were embedded with epoxy resin, and polished using 600#, 1200#, 2500# and 4000#- grits silicon carbide (SiC) abrasive papers under continuous water irrigation (30s each paper-step) **(Figure 1)**. Afterwards, the specimens were submitted to Knoop Hardness number (KHN) assessment. KHN1 measurements were performed on the irradiated surface (upper) using an indenter (Duramin 2, Ballerup, Denmark), under a load of 25 gf for 15 s. In each sample, five measurements were obtained from the upper surface and means were obtained.

Thereafter, the specimens were immersed in 20 ml absolute ethanol for 24 h to evaluate the softening ratio and the elution of monomers by KHN mean (Schneider *et al.*, 2008) (**Figure 1**). Subsequently, new Knoop hardness (KHN2) measurements were obtained, as aforementioned. The softening ratio (hardness decrease percentage) was obtained. The rate of softening was determined using the following formula: 100 – (KHN2/KHN1 x 100).

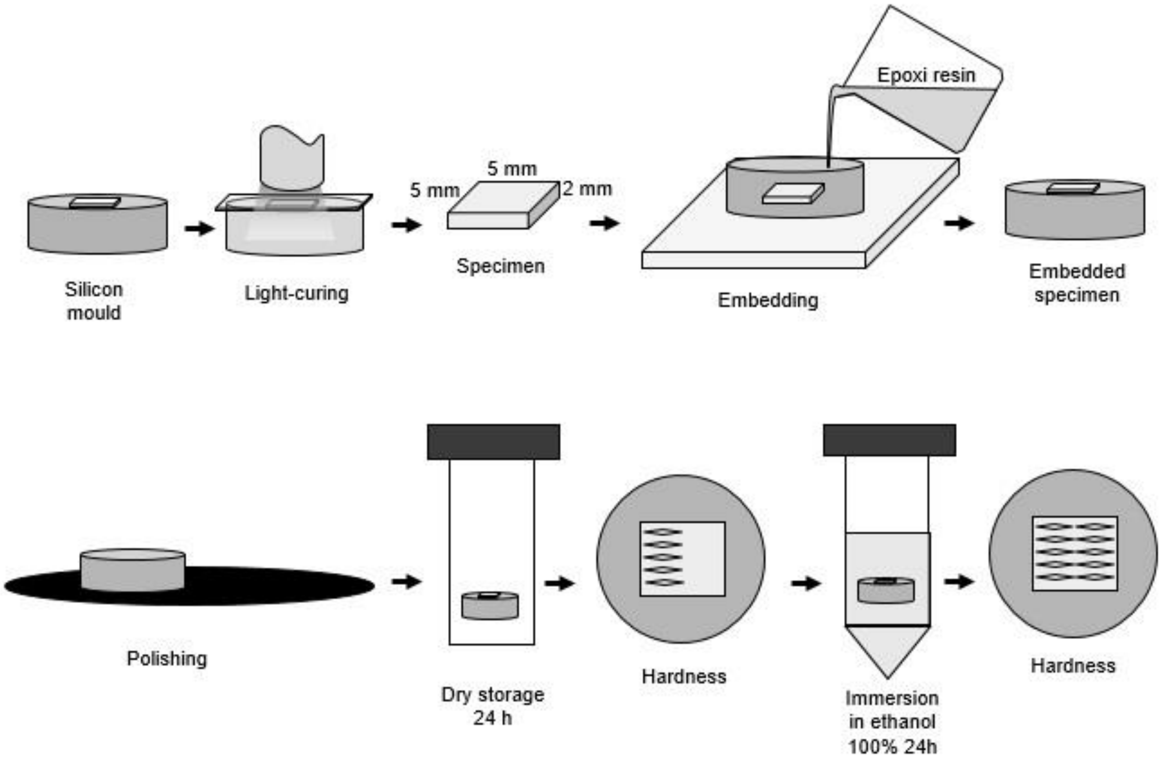

Figure 1. Representative scheme showing the specimen confection, followed by the embedding in epoxy resin. After, the polishing of the specimens, immersion in distilled water for 24 h, and the initial hardness measurements. Then, specimens were immersed in ethanol 100% for 24 h, and the final hardness measurements.

2.4. Tensile Cohesive Strength (TCS)

Silicon moulds were confectioned in the halter shape (2 mm height X 8 mm length X 1.5 mm constriction region). The materials were inserted into each mould in order to fill it completely. The material surface was covered with a polyester strip (Mylar strip, Keystone Ind. GmbH, Singen, Germany) and pressed with a glass slide to squeeze out any excess of material before the light-curing procedures. The specimens were light-cured using a halogen light photo activator at 600 mW/cm^2 for 60 s (Optilux VLC; Demetron, CT, USA). After, the halter shaped specimens were removed from the moulds and hand-polished under irrigation using 400#, 600# and 1200# grits silicon carbide (SiC) abrasive papers. Ten specimens were produced for each group (n=10). After storage for 24 h, specimens were fixed on a device with cyanoacrylate (Super Bonder gel, Loctite, Henkel Corp, Rocky Hill, CT, USA) and tested up to the failure under tensile using a universal testing machine (Instron, Model 5569A, High Wycombe, UK) with load cell 500N, at a crosshead speed of 0.5 mm/min (**Figure 2**). The exact measurement of the transversal section of the fractured specimens was measured with a digital caliper. TCS was calculated in MPa.

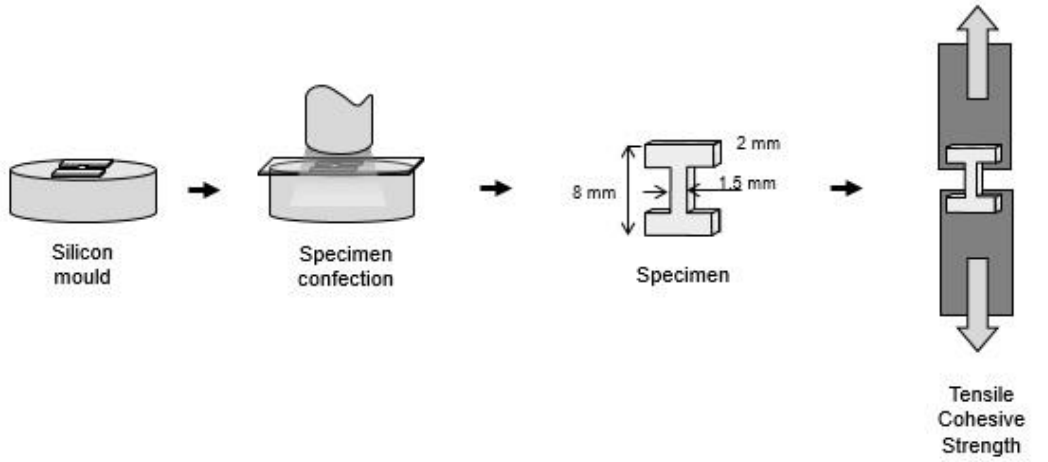

Figure 2. Representative image showing the specimens confection, size and Tensile Cohesive Strength.

2.5. Flexural Strength (FS) (3 points bending) and Elastic Modulus (E-Modulus)

Seventy rectangular bars specimens with standardized dimensions (2 mm width X 2 mm thickness X 7 mm length) were obtained according to the ISO 4049 protocol (except for specimens dimensions) (n=10). The resin infiltrant materials were inserted into each mould and the upper surface was covered with a polyester strip (Mylar strip, Keystone Ind. GmbH, Singen, Germany) and pressed with a glass slide to squeeze out any excess of material before light-curing procedures. The specimens were light-cured at 600 mW/cm^2 for 60 s (Optilux VLC; Demetron, CT, USA). The specimens were stored for 24 h into distilled water at 37ºC. After storage, 3 points flexural strength was evaluated, with speed 0.5 mm/min, using a universal testing machine Instron (Model 5569A, High Wycombe, UK). The FS was monitored by the software Bluehill 2 (Instron Corporation, High Wycombe, UK) in a computer attached to the testing machine that allowed to obtain the *E*-Modulus and flexural modulus.

2.6. Water sorption (WS) and solubility (SL)

Water sorption and solubility were obtained according to ISO 4049/2000, except for the dimensions of specimens which were modified in order to the specimen size was similar to the light-curing device tip. Specimens with 6.0 ± 0.1 mm in diameter and 1.0 ± 0.1 mm in thickness (n=5) were made in a silicon mould. Infiltrants were inserted in the mould and light-cured at 1000 mW/cm^2 for 40 s (Ultralume 5; Ultradent, South Jordan, Utah, USA). Immediately after light-curing, the specimens were placed in a desiccator and transferred to a pre-conditioning oven at 37ºC. The specimens were repeatedly weighed after 24 h intervals until a constant mass (m_1) was obtained (variation was less than 0.2 mg in any 24 h period). Thickness and diameter of the specimens were measured using a digital caliper, from the mean of four equidistant points, and these measurements were used to calculate the volume (V) of each specimen (mm^3).

They were then individually placed in sealed glass vials containing 10 mL of distilled water at 37ºC for 7 days period. After, the specimens were washed in running water, gently wiped with a soft absorbent paper, weighed in an analytical balance (m_2) and returned to the vials containing 10 mL of fresh distilled water. Following the 7-days of storage, the specimens were dried inside a desiccator containing fresh silica gel and weighed daily until a constant mass (m_3) was obtained (as previously described). The initial mass determined after the first desiccation process (m_1) was used to calculate the change in mass after each time interval, during the 7 days of storage in water. Changes in mass were plotted against the storage time in order to obtain the kinetics of water absorption during the entire period of water storage. Water sorption (WS - $\mu g/mm^3$) and solubility (SL - $\mu g/mm^3$) over the 7-days of water storage were calculated using the following formulae:

$$WS = (m_2 - m_3/V_0)$$

$$SL = (m_1 - m_3/V_0)$$

2.7. Statistical analysis

Data from degree of conversion (DC), Knoop hardness number (KHN1), Knoop hardness number (after immersion in ethanol) (KHN2), softening ratio (SR), tensile cohesive strength (TCS), flexural strength (FS), elastic modulus (*E*-Modulus) and water sorption (WS) and solubility (SL) were submitted to one-way ANOVA and Tukey's test (α=0.05).

3. RESULTS

Results of degree of conversion (DC), Knoop Hardness number (KHN1), softening ratio (SR), tensile cohesive strength (TCS), flexural strength (FS) and elastic modulus (*E*-Modulus) for the infiltrant materials are shown in **Table 2.** For DC, T+B, ACP, BAG 45S5 and HCAT-β were similar among them. However, T+B showed no statistically difference when compared to HAp and BAG 45S5 as well. HAp was statistically similar to BAG Zn. All the experimental infiltrants showed significant statistically difference when compared to ICON®. Regarding to the KHN1, there was no significant statistically differences among the infiltrants containing bioactive particles except for BAG 45S5 (HAp, ACP, BAG Zn and HCAT-β). T+B showed statistically difference when compared to the experimental infiltrants containing bioactive particles. Also, ICON® showed statistically difference when compared to all the experimental materials. The softening ratio of the infiltrants showed no statistical differences among the experimental infiltrants containing bioactive particles (HAp, ACP, BAG Zn, BAG 45S5 and HCAT-β). T+B was statistically different to HAp, however, it was similar to the other experimental infiltrants (ACP, BAG Zn, BAG 45S5 and HCAT-β). ICON® showed statistically difference when compared to all the experimental infiltrants. Regarding to the TCS, there was no statistical difference among the experimental infiltrants (T+B, HAp, ACP, BAG Zn, BAG 45S5 and HCAT- β); however, BAG Zn showed no significant statistically difference when compared to ICON®. For the FS, the outcomes showed that there was no significant statistically difference among the experimental infiltrants T+B, HAp, ACP and BAG 45S5. Also, HAp, ACP and BAG 45S5 were similar to BAG Zn. Otherwise, BAG Zn, HAp and BAG 45S5 did not show statistical difference to HCAT-β. HCAT-β and ICON® were statistically similar between them. Regarding to the *E*-Modulus, there was no statistically difference among all the experimental infiltrants (with or without the addition of bioactive particles), however, HAp, BAG Zn, BAG 45S5 and HCAT-β were statistically similar to ICON® as well.

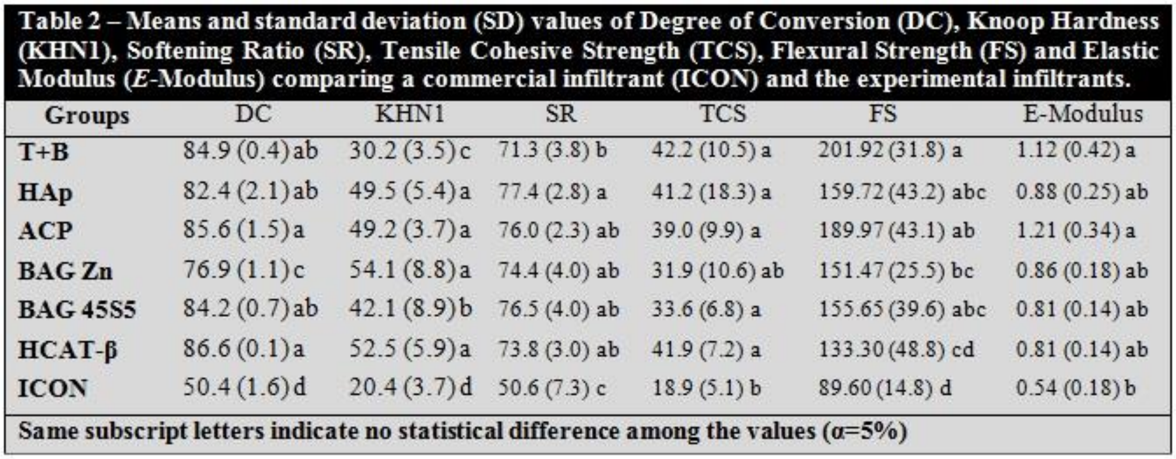

Table 2 – Means and standard deviation (SD) values of Degree of Conversion (DC), Knoop Hardness (KHN1), Softening Ratio (SR), Tensile Cohesive Strength (TCS), Flexural Strength (FS) and Elastic Modulus (*E*-Modulus) comparing a commercial infiltrant (ICON) and the experimental infiltrants.

Groups	DC	KHN1	SR	TCS	FS	E-Modulus
T+B	84.9 (0.4) ab	30.2 (3.5) c	71.3 (3.8) b	42.2 (10.5) a	201.92 (31.8) a	1.12 (0.42) a
HAp	82.4 (2.1) ab	49.5 (5.4) a	77.4 (2.8) a	41.2 (18.3) a	159.72 (43.2) abc	0.88 (0.25) ab
ACP	85.6 (1.5) a	49.2 (3.7) a	76.0 (2.3) ab	39.0 (9.9) a	189.97 (43.1) ab	1.21 (0.34) a
BAG Zn	76.9 (1.1) c	54.1 (8.8) a	74.4 (4.0) ab	31.9 (10.6) ab	151.47 (25.5) bc	0.86 (0.18) ab
BAG 45S5	84.2 (0.7) ab	42.1 (8.9) b	76.5 (4.0) ab	33.6 (6.8) a	155.65 (39.6) abc	0.81 (0.14) ab
HCAT-β	86.6 (0.1) a	52.5 (5.9) a	73.8 (3.0) ab	41.9 (7.2) a	133.30 (48.8) cd	0.81 (0.14) ab
ICON	50.4 (1.6) d	20.4 (3.7) d	50.6 (7.3) c	18.9 (5.1) b	89.60 (14.8) d	0.54 (0.18) b

Same subscript letters indicate no statistical difference among the values (α=5%)

Water sorption (WS) and solubility (SL) means and standard deviation are presented in **Table 3**. ICON® did not show significant statistically difference when compared to ACP and BAG 45S5. Also, ACP and BAG 45S5 were similar to T+B, BAG Zn and HCAT- β. However, T+B, BAG Zn, BAG 45S5 and HCAT-β were statistically similar to HAp. The outcomes of the SL showed that ICON® was statistically similar to ACP. ACP, otherwise, showed no statistically difference when compared to HCAT-β. There was no significant statistically difference among T+B, HAp, BAG Zn, BAG 45S5 and HCAT-β.

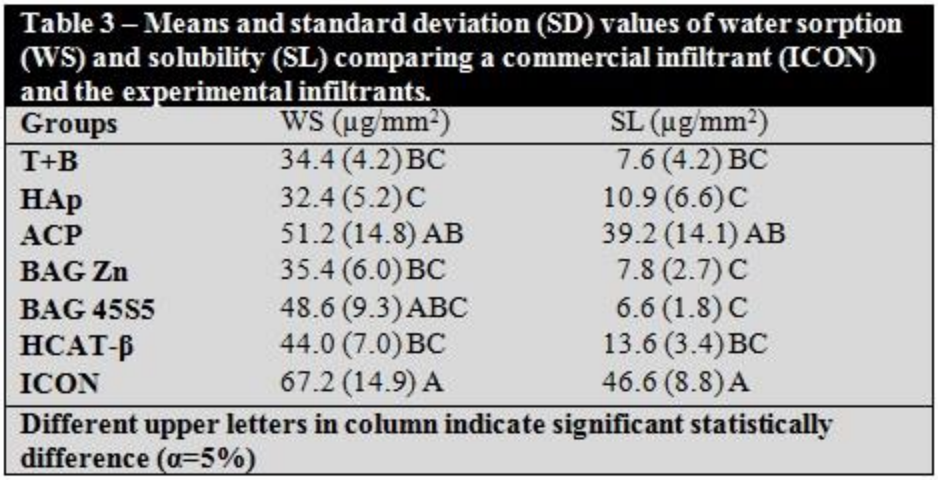

Table 3 – Means and standard deviation (SD) values of water sorption (WS) and solubility (SL) comparing a commercial infiltrant (ICON) and the experimental infiltrants.

Groups	WS (µg/mm²)	SL (µg/mm²)
T+B	34.4 (4.2) BC	7.6 (4.2) BC
HAp	32.4 (5.2) C	10.9 (6.6) C
ACP	51.2 (14.8) AB	39.2 (14.1) AB
BAG Zn	35.4 (6.0) BC	7.8 (2.7) C
BAG 45S5	48.6 (9.3) ABC	6.6 (1.8) C
HCAT-β	44.0 (7.0) BC	13.6 (3.4) BC
ICON	67.2 (14.9) A	46.6 (8.8) A

Different upper letters in column indicate significant statistically difference (α=5%)

4. DISCUSSION

Overall, this study found that the experimental infiltrants (with or without the addition of bioactive particles) showed better chemical and mechanical properties when compared to an available commercially infiltrant (ICON®), except for the softening ratio test which ICON® presented the lower percentage, indicating a high cross-link density. In this way, the hypothesis tested in this study was accepted for some chemical and mechanical properties such as degree of conversion, Knoop hardness, tensile cohesive strength, flexural strength, *E*-Modulus, and water sorption and solubility, but rejected for the softening ratio test. A high degree of conversion of the organic matrix is often related to superior mechanical properties in composite restorative materials, decreasing the risk of fracture and wear while in function (Ferracane and Greener, 1986; Bouschlicher *et al.,* 2004). Dimethacrylate copolymerization through light or heat activation in the presence of an initiator results in a cross-linked polymer whose physical-chemical properties depend on the degree of conversion (DC) and final network structure (Asmussen and Peutzfeldt, 1998). The molecular structure of BisEMA (bisphenol A ethoxylated dimethacrylate) monomer is almost the same of BisGMA (bisphenol A glycidyl methacrylate) monomer, except for the absence of hydroxyl groups. It shows higher molecular weight than ethylene glycol derivate but its viscosity is low as well, due to the absence of hydroxyl groups that form hydrogen bondings. In this manner, the lower viscosity reduces the maximum rate of polymerization, and enhances the final conversion achieved by the polymer (Gajewski *et al.,* 2012; Sideridou *et al.,* 2002), and allows for higher DC and better mechanical properties to be achieved (Ogliari *et al.,* 2008). Regarding to TEGDMA (triethylene glycol dimethacrylate), an important feature is that the flexible TEGDMA improves conversion (Pfeifer *et al*., 2011; Cramer *et al.,* 2011) and crosslinking (Pfeifer *et al.,* 2011; Sideridou *et al.,* 2002) , resulting in fewer leachable components (Floyd and Dickens, 2006). Thus, the monomer structures may explain the results obtained in this study, which showed higher DC for the experimental infiltrants when compared to ICON®. The lower DC found to ICON® could be explained due to the high presence of only TEGDMA in its composition. Earlier studies (Sideridou *et al.,* 2002; Lovell *et al.,* 1999a; Dickens *et al.,* 2003) showed that, as the concentration of TEGDMA increases to over 70 mol%, there is a trend for decreased conversion, probably due to greater cyclization at higher TEGDMA content. Moreover, Belli *et al.* (2014) showed that the incorporation of nanoparticles fillers in a particular self-etching monomer mixture had the potential to promote the strengthening of the adhesive resin and the adhesive interface, with improvements to the degree of conversion and polymerization efficacy. Particularly, Park *et al.* (1998) studied ACP composites in a previous work. Results of the mentioned study showed that ACP composites have mechanical properties that are probably adequate for application as base/liner materials and possibly as sealants as well. Although it has not been studied in an infiltrant material, but it showed promisor results for sealants, it is possible to make an analogy with our findings, as we showed adequate properties for ACP-based experimental infiltrants. Also, a previous study showed that adding HAp particles about 10 µm in diameter to a conventional restorative glass ionomer cement (GIC) indicated that HAp functions as an adsorbent and an ion exchangeable agent, rather than as reinforcement, resulting in improved mechanical and chemical properties of GIC (Arita *et al.*, 2011). In this manner, we believe that the addition of bioactive particles into the experimental infiltrants keeps the DC with higher values than ICON®, showing adequate values of mechanical properties. Also, high DC of the experimental infiltrants when compared to ICON® may explain the results obtained for Knoop hardness (KHN), tensile cohesive strength (TCS), flexural strength (FS) and elastic modulus (*E*- Modulus), as high DC values lead to an improvement of the mechanical properties (Ferracane and Greener, 1986; Bouschlicher *et al.,* 2004).

The polymerization of methacrylate results in a highly crosslinked structure. Monomer conversion, however, is never complete, and the polymer contains considerable quantities of remaining, unreacted double bonds (Ferracane *et al.*, 1997). The quantity of remaining double bonds depends on the monomer mixture composition, the nature of the initiatior system (Asmussen, 1982; Ferracane and Greener, 1986), and on the amount of activating light (Condon and Ferracane, 1997; Silikas *et al.,* 2000). Polymerization varies not only with the curing light intensity (Silikas *et al.*, 2000; Davidson-Kaban *et al.*, 1997; Watts and Hindi, 1999), but also with the composition of the polymerizing material.

Storage in ethanol was used as the method to disclose differences in polymer structure. The storage in ethanol is an indirect method of polymer softening after immersion in organic solvents used to estimate crosslinking density and evaluate tri-dimensional network formation, however, this method provides limited information, since it relies on other factors, such as the solubility parameters of the material and solvent. According to this method, it is inevitable that a certain amount of the polymeric material (unreacted monomer, oligomers, and linear polymer) is extracted into the ethanol (Ferracane, 1994). Thus, we supposed that the bioactive particles and certain amount of the polymeric material from the experimental infiltrant (T+B) may have been leached during the period of storage in ethanol, which could contribute for the higher softening ratio (SR) for all the experimental infiltrants (with or without bioactive particles). ICON® showed a lower initial Knoop hardness (KHN1) value regarding to all the experimental infiltrants, which could be explained due to the absence of bioactive particles and BisEMA and the presence of a great amount of TEGDMA in its composition. The lower softening ratio presented for ICON® could be explained exactly due to the greater amount of TEGDMA in its composition. The fact that TEGDMA has three ether linkages from the glycol group (not sterically hindered from a stiff backbone) besides the two carbonyls from the methacrylate (Lemon *et al.,* 2007), makes it a more efficient hydrogen bond acceptor than BisEMA which presents the ether linkages and the methacrylate carbonyls shielded by a large, relatively stiff molecule. A previous study showed that at

TEGDMA concentrations higher than 40 mol%, the lower initial viscosity and the greater tendency towards cyclization during polymerization combine to extend the amount of network formation necessary to reach the mobility limitation threshold that allows effective autoacceleration. Cyclization contributes to conversion, but not to overall network development and leads to heterogeneity (Lovell *et al.*, 1999b; Poshusta *et al.*, 2002). Cyclic structures provide enhanced overall mobility, as well as increase the mobility of pendant groups and crosslinks, with an effect analogous to plasticizers (Lovell *et al.*, 1999b). Pfeifer *et al.* (2011) also showed that higher TEGDMA contents in the gel portion, as well as higher limiting conversion, result in lower free volume loss after extraction (even though in the case of TEGDMA-rich mixtures the overall free volume might be higher because of the greater freedom to rotation associated with these molecules), pointing to the expected increase in crosslinking density.

Most of the monomers used in dental resin materials can absorb water and chemicals from the environment, and also release components into the surrounding environment (Santerre *et al*., 2001; Ferracane, 2004). Both water sorption and solubility would lead to a variety of chemical and physical processes that may result in deleterious effects on the structure and function of dental polymers (Malacarne *et al*., 2006). The longevity of dental restorations is related to the quality of the polymer formed (Ferracane, 2006). The addition of filler decreases the relative amount of polymeric matrix, decreasing the contraction stress (Condon and Ferracane, 2000) and hydrolytic degradation (Andrzejewska, 2001). In this study, all the experimental infiltrants (with and without the addition of bioactive particles) showed a lower water sorption compared to the commercial infiltrant ICON®, except ACP which showed a similar statistical value to ICON® as well. This fact might be explained due to the composition of the materials. In general terms, water sorption correlates with the conversion achieved by the polymer and also the nature of the formed network, both in terms of its relative hydrophilicity, and the tridimensional structure and free volume (Pfeifer *et al.*, 2011). An earlier study showed that the water sorption increased with the decrease in conversion (Gajewski *et al.*, 2012). As aforementioned, we obtained lower degree of conversion for ICON® than the experimental infiltrants, which could explain the lower

KHN1, TCS, FS and *E*-Modulus and the higher water sorption obtained for ICON®, in this study. The lower water sorption of the experimental infiltrant T+B compared to ICON® could be explained due to the presence of BisEMA in its composition, which corroborates with a previous study that showed lowest water sorption for BisEMA, due to the relatively high conversion and to the hydrophobic character of the molecule (Lemon *et al.*, 2007).

Regarding to the solubility of the tested materials, ICON® and ACP presented higher solubility when compared to the other groups. The behavior of ACP might be related to the particle size used in this study. ACP was the only group with the addition of nano-sized particles. The solubility tends to increase when the particle size decreases, because the area ratio of the surface per volume becomes higher, which facilitates the dissolution reaction in a water environment. Earlier studies showed that this fact is determinant to the solubility when phosphate is found in simulated body fluid (Bertazzo, 2004). Comparing the particle size of ACP with BAG Zn and BAG 45S5, we could note a difference among them, which could generate a higher surface area of the particles for ACP, explaining the discrepancies found in the solubility levels of the materials. The high solubility presented for ICON® might be due to the high amount of TEGDMA in its composition. Gajewski *et al.* (2012) showed that TEGDMA, due to the tendency to cyclization, presented the highest solubility results, probably because low-molecular-weight oligomers were present and ready to leach. On the other hand, the lowest solubility values from BisEMA were explained by both the relatively high conversion and the hydrophobic character of the molecule. These findings are essential to guide the formulation of future remineralizing infiltrants which should remineralize the infiltrated and adjacent enamel besides to hamper the lesion progression. Further studies are already in progress to evaluate the penetration and the potential remineralization of the tested experimental infiltrants.

5. CONCLUSION

It can be concluded that the experimental resin infiltrants presented better performance regarding the chemical-mechanical properties than the commercial infiltrant ICON®. The addition of bioactive particles in the experimental materials improved their chemical and mechanical properties when compared to a commercial material ICON®.

6. ACKNOWLEDGEMENTS

The authors thank Capes-Brazil for the research grant 3352-13-7, and DMG from Brazil for providing ICON® kits.

7. REFERENCES

1. Andrzejewska E. Photopolymerization kinetics of multifunctional monomers. Prog in Polym Sci 2001;26:605-65.
2. Arita K, Yamamoto A, Shinonaga Y, Harada K, Abe Y, Nakagawa K, Sugiyama S. Hydroxyapatite particle characteristics influence the enhancement of the mechanical and chemical properties of conventional restorative glass ionomer cement. Dent Mater J 2011; 30(5): 672-683.
3. Asmussen E. Factors affecting the quantity of remaining double bonds in restorative resin polymers. Scand J Dent Res 1982;90:490-496.
4. Asmussen E, Peutzfeldt A. Influence of UEDMA, BisGMA and TEGDMA on selected mechanical properties of experimental resin composites. Dent Mater 1998;14:51-56.
5. Asmussen E, and Peutzfeldt A. A influence of pulse-delay curing on softening of polymer structures. J Dent Res 2001; 80:1570-1573.
6. Atai M, Nekoomanesh M, Hashemi SA, Amani S. Physical and mechanical properties of an experimental dental composite based on a new monomer. Dent Mater 2004;20:663-8.

7. Belli R, Kreppel S, Petschelt A, Hornberger H, Boccaccini AR, Lohbauer U. Strengthening of dental adhesives via particle reinforcements. J Mech Behav Biomed Mater 2014;37:100-108.
8. Bertazzo S, Bertran CA. Solubilidade de fosfatos de cálcio em fluído corpóreo simulado. Biocompatibilidade e propriedades da interface fosfato de cálcio/solução. UNICAMP 2004.
9. Bonilla ED, Yashar M, and Caputo AA. Fracture toughness of nine flowable resin composites. J Prosthet Dent 2003; 89:261-267.
10. Bouschlicher MR, Rueggeberg FA, Wilson BM. Correlation of bottom-to-top surface microhardness and conversion ratios for a variety of resin composite compositions. Oper Dent 2004;29(6):698-704.
11. Condon JR, Ferracane JL. In vitro wear of composites with varied cured, filler level, and filler treatment. J Dent Res 1997;76:1405-1411.
12. Condon JR, Ferracane JL. Assessing the effect of composite formulation on polymerization stress. J Am Dent Assoc 2000;131:497-503.
13. Cramer NB, Stansbury JW, Bowman CN. Recent advances and developments in composite dental restorative materials. J Dent Res 2011;90(4):402-16.
14. Davidson-Kaban SS, Davidson CL, Feilzer AJ, De Gee AJ, Erdilek N. The effect of curing light variations on bulk curing and wall-to-wall quality of two types and various shades of resin composites. Dent Mater 1997;13:344-352.
15. Dickens S, Stansbury J, Choi K, Floyd C. Photopolymerization kinetics of methacrylate dental resins. Macromol 2003;36:6043-6053.
16. Ekstrand KR, Bakhshandeh A, Martignon S. Treatment of proximal superficial caries lesions on primary molar teeth with resin infiltration and fluoride varnish versus fluoride varnish only: efficacy after 1 year. Caries Res 2010;44(1):41-6.
17. Featherstone JD. Caries prevention and reversal based on the caries balance. Pediatr Dent 2006;28:128-32.
18. Ferracane JL, Greener EH. The effect of resin formulation on the degree of conversion and mechanical properties of dental restorative resins. J Biomed Mater Res 1986;20:121-131.

19. Ferracane JL, Mitchem JC, Condon JR, Todd R. Wear and marginal breakdown of composites with various degrees of cure. J Dent Res 1997;76:1508-1516.
20. Ferracane JL. Elution of leachable components from composites. J Oral Rehabil 1994;21(4):441-52.
21. Ferracane JL. Hygroscopic and hydrolytic effects in polymer networks. In: Proceedings of conference on scientific insights into dental ceramics and photopolymer networks, vol. 18. 2004. P. 118-28.
22. Ferracane JL. Hygroscopic and hydrolytic effects in dental polymer networks. Dent Mater 2006;22:211-22.
23. Floyd CJ, Dickens SH. Network structure of BisGMA- and UDMA-based resin systems. Dent Mater 2006;22(12):1143-9.
24. Gajewski VE, Pfeifer CS, Fróes-Salgado NR, Boaro LC, Braga RR. Monomers used in resin composites: degree of conversion, mechanical properties and water sorption/solubility. Braz Dent J 2012;23(5):508-514.
25. Guiraldo RD, Consani S, Consani RL, Berger SB, Mendes WB and Sinhoreti MA. Light energy transmission through composite influenced by materials shades. Bull. Tokyo Dent Coll 2009; 50: 183-190.
26. Hirayama S, Iwai H, Tanimoto Y. Mechanical evaluation of five flowable resin composites by the dynamic micro-indentation method. J Dent Biomechanics 2014; 5:1-8.
27. Langhorst SE, O'Donnell JNR, Skrtic D. *In vitro* remineralization of enamel by polymeric amorphous calcium phosphate composite: Quantitative microradiographic study. Dent Mater 2009;25:884-891.
28. Lemon MT, Jones MS, Stansbury JW. Hydrogen bonding interactions in methacrylate monomers and polymers. J Biomed Mater Res Part A 2007;83A:734-746.
29. Lovell LG, Stansbury JW, Syrpes DC, Bowman CN. Effects of composition and reactivity on the reactions kinetics of dimethacrylate/dimethacrylate copolymerizations. Macromol 1999a;32:3913-21.

30. Lovell LG, Newman SM, Bowman CN. The effects of light intensity, temperature, and comonomer composition on the polymerization behavior of dimethacrylate dental resins. J Dent Res 1999b; 78(8): 1469-1476.
31. Lynch RJM, Smith SR. Remineralization agents: New and effective or just marketing hype? Adv Dent Res 2012;24:63.
32. Malacarne J, Carvalho RM, de Goes MF, Svizero N, Pashley DH, Tay FR, Yiu CK, Carrilho MR. Water sorption/solubility of dental adhesive resins. Dent Mater 2006;22:973-980.
33. Martignon S, Ekstrand KR, Gomez J, Lara JS, Cortes A. Infiltrating/sealing proximal caries lesions: a 3-year randomized clinical trial. J Dent Res 2012;91(3):288-92.
34. Meyer-Lueckel H, Bitter K, Paris S. Randomized controlled clinical trial on proximal caries infiltration: three-year follow-up. Caries Res 2012;46(6):544-8.
35. Ogliari FA, Ely C, Zanchi CH, Fortes CB, Samuel SM, Demarco FF, et al. Influence of chain extender length of aromatic dimethacylates on polymer network development. Dent Mater 2008;24:165-171.
36. Paris S, Meyer-Lueckel H, Kielbassa AM. Resin infiltration of natural caries lesions. J Dent Res 2007;86(7):662-666.
37. Paris S, Meyer-Lueckel H. Infiltrants inhibit progression of natural caries lesions *in vitro*. J Dent Res 2010;89(11):1276-80.
38. Park MS, Eanes ED, Antonucci JM, Skrtic D. Mechanical properties of bioactive amorphous calcium phosphate/methacrylate composites. Dent Mater 1998;14:137-141.
39. Pfeifer CS, Shelton ZR, Braga RR, Windmoller D, Machado JC, Stansbury JW. Characterization of dimethacrylate polymeric networks: a study of the crosslinked structure formed by monomers used in dental composites. Eur Polym J 2011;47(2):162-70.
40. Poshusta AK, Bowman CN, Anseth KS. Application of a kinetic gelation simulation to the characterization of in situ cross-linking biomaterials. J Biomat Scie-Polymer Edition. 2002; 13(7): 797-815.

41. Robinson C, Weatherell JA, Kirkham J, 1995. The chemistry of dental caries. In: Robinson C, Kirkham J, Shore RC (Eds), Dental Enamel Formation to Destruction. CKC Press, New York, pp 223-243.
42. Rueggeberg FA, Hashinger DT, Fairhurst CW. Calibration of FTIR conversion analysis of contemporary dental resin composites. Dent Mater 1990;6:241-9.
43. Santerre JP, Shajii L, Leung BW. Relation of dental composite formulations to their degradation and the release of hydrolyzed polymeric-resin-derived products. Crit Rev Oral Biol Med 2001;12:136-51.
44. Schneider LF, Moraes RR, Cavalcante LM, Sinhoretti MA, Correr-Sobrinho L, Consani S. Cross-link density evaluation through softening test: Effect of ethanol concentration. Dent Mater 2008;24:199-203.
45. Sideridou I, Iserki V, Papanastasiou G. Effect of chemical structure on degree of conversion in light-cured dimethacrylate-based dental resins. Biomater 2002;23(8):1819-29.
46. Sideridou I, Tserki V, Papanastasiou G. Study of water sorption, solubility and modulus of elasticity of light-cured dimethacrylate-based dental resin. Biomater 2003;24:655-665.
47. Silikas N, Eliades G, Watts DC. Light intensity effects on resin-composite degree of conversion and shrinkage strain. Dent Mater 2000;16:292-296.
48. Siverstone LM. Remineralization phenomena. J Caries Res 1977;11(suppl):59-84.
49. St-Georges AJ, Swift EJ Jr., Thompson JY, *et al.* Irradiance effects on the mechanical properties of universal hybrid and flowable hybrid resin composites. Dent Mater 2003; 19:406-413.
50. Sumino N, Tsubota K, Takamizawa T, *et al.* Comparison of the wear and flexural characteristics of flowable resin composites for posterior lesions. Acta Odontol Scand 2013; 71:820-27.
51. Ten Cate JM, Larsen MJ, Pearce EIF, Fejerskov O, 2003. Chemical interactions between the tooth and oral fluids. In: Fejerskov O, Kidd EAM (Eds). Dental Caries. Blackwell Munksgaard, Oxford, pp 49-69.

52. Watts DC, Hindi AA. Intrinsic “soft-start” polymerization shrinkage-kinetics in an acrylate-based resin composite. Dent Mater 1999;15:39-45.
53. Yap AU, Soh MS, Han TT, Siow KS. Influence of curing lights and modes on cross-link density of dental composites. Oper Dent 2004;29:410-415.

CAPÍTULO 2

Penetration and Knoop hardness depth of experimental infiltrants materials incorporated with bioactive particles in enamel subsurface lesion

ABSTRACT

Objective: The aim of this study was to evaluate the brushing abrasion (surface roughness before and after brushing abrasion), the Knoop hardness depth of the materials after a pH cycling (1 month) by microhardness analysis and the ability of experimental infiltrants incorporated with bioactive particles to penetrate into artificial caries-like lesion.

Methods: Groups were set up as follows: T+B (TEGDMA 75 wt% + BisEMA 25 wt%); HAp (T+B+ Hydroxyapatite 10 wt%); ACP (T+B+ amorphous calcium phosphate 10 wt%); BAG Zn (T+B+ bioactive glass Zn 10 wt%); BAG 45S5 (T+B+ bioactive glass 45S5 10 wt%); HCAT-β (T+B+ β-TCP modified calcium silicate cements 10 wt%) e ICON®. Specimens were comprised by each group for the following tests: roughness before and after brushing abrasion (n=10), microhardness (n=10), and Confocal Laser Scanning Microscopy (CLSM) (n=5). Caries-like lesions were made in thirty and five sound human molars for CLSM each and in eighty for microhardness. For microhardness analysis, a carious group (n=10) was included. Roughness and microhardness were evaluated by two-way repeated measure ANOVA and Tukey's test (α=0.05). The penetration ability of resin infiltrants on caries-like lesions was analyzed by Confocal Microscopy.

Results: ACP showed the lower surface roughness before and after brushing abrasion. BAG Zn, BAG 45S5 and HCAT-β showed superior values when compared to all the other groups. However, all the groups tested were statistically higher than carious group. For micro-hardness, all the tested infiltrants were statistically higher than carious group; however, BAG Zn, BAG 45S5 and HCAT-β showed higher values when compared to the other materials.

Confocal microscopy showed that all groups showed a regular and good penetration into the caries-like lesions, except ACP.

Conclusion: ACP showed the best results for surface roughness before and after brushing cycle. All the infiltrants tested showed increased micro-hardness after pH cycling. Also, the materials showed a good penetration into the enamel lesion body for all materials, except for ACP, according to confocal analysis.

Key-words: hydroxyapatite, elastic modulus, confocal microscopy, brushing

1. INTRODUCTION

Acid-producing bacteria in the biofilm diffuse into the tooth and dissolve the carbonated hydroxyapatite mineral, forming a caries lesion (Silverstone, 1973). If this process continues, cavitation results. Prior to cavitation, a subsurface lesion with partial demineralization is present, and this can be remineralized (Featherstone, 2009). According to the modern concept of dental caries management, prevention and hard-tissue preservation are the primary goals, and dentists are encouraged to prefer a more conservative and biological rather than a surgical approach (Steinberg, 2002). Common non-invasive treatment for enamel caries includes fluoride application, sealants and behavioral modification. For pits and fissures, mainly on the occlusal surfaces of permanent molars, sealing the occlusal surfaces of permanent molars, sealing with light-curing resins has been shown to be an effective preventive measure (Mejare *et al.*, 2003; Ahovuo-Saloranta *et al.*, 2008). However, dental sealants and adhesives are not optimized for high penetrability and have therefore shown only superficial penetration into natural enamel lesions (Paris *et al.*, 2007).

Several studies have been shown the efficacy of the infiltration in enamel subsurface caries lesion using an available commercially material ICON® (Paris and Meyer-Lueckel, 2009; Paris and Meyer-Lueckel, 2010, Paris *et al.*, 2010; Phark *et al.*, 2009). ICON® has been used as an alternative therapy for the arrest of caries lesions as an infiltration of subsurface lesions with low-viscous light-curing resins, and has an extremely high penetration coefficient that facilitates deeper penetration. Caries infiltration aims to occlude the pathways since porosities of enamel caries act as diffusion pathways for acids and dissolved minerals, and thus, leading to an arrest of caries progression (Paris *et al.*, 2007). A recent study showed that the use of conventional infiltration technique for proximal and smooth surface lesions seems to result in lower penetration depths when used for fissure caries lesions (Lausch *et al.*, 2015). However, the latter study used the conventional infiltrant commercially available (ICON®, DMG, Hamburg, Germany).

The incidence of demineralized enamel surfaces is gradually increasing in the public. Not only orthodontic treatment but also daily food habits can cause enamel demineralization (Gorelick *et al.*, 1982; Tufekci *et al.*, 2011). Many clinical products have been developed to improve enamel remineralization, including fluoride varnish (Marinho *et al.*, 2013), fluoride dentifrice (Tschoppe and Meyer-Lueckel, 2012), and casein phosphopeptide-amorphous calcium phosphate (CPP-ACP) paste (Cao *et al.*, 2013). Although CPP-ACP can promote remineralization of subsurface enamel lesions, the crystals formed were loosely structured and morphologically irregular after treatment with these agents (Fan *et al.*, 2011). Therefore, studies were performed to explore enamel remineralization through biomimetics (Zhou *et al.*, 2012).

The remineralization might be described as the delivery of calcium and phosphate, from outside the tooth, into the enamel lesion, effecting deposition of mineral onto the demineralized enamel within (Lynch and Smith, 2012). In that way, the infiltrant needs bioactive particles in its composition so that the remineralization process can occur.

Nowadays, several studies (Reynolds, 2008; Rao and Malhotra, 2011; Reynolds *et al*, 2009; Cochrane *et al*, 2010; Banerjee *et al*, 2011) have been carried out in order to seek minimal intervention approaches, i.e., focuses on the least invasive treatment options possible in order to minimize tissue loss and patient discomfort (Rao and Malhotra, 2011). Thus, concentrating mainly on prevention and early intervention of caries, minimal intervention first basic principle is the remineralization of early carious lesions, advocating a biological or therapeutic approach rather than the traditional surgical approach for early surface lesions (Rao and Malhotra, 2011).

Different materials are used to remineralize tooth substrate such as hydroxyapatite, amorphous calcium phosphate, bioactive glass zinc, bioactive glass 45S5 and β-tricalcium phosphate modified calcium silicate cements. Nevertheless, there are no studies about the use of these bioactive particles into resin infiltrants.

A previous study showed that restorations with smooth surfaces are important to inhibit plaque accumulation (de Fucio *et al*., 2009). Surface degradation of resin materials restoration can occur because of the presence of chemicals from food and drinks in the oral environment, resulting in unaesthetic appearance and increased surface roughness, accelerating the wear of dental materials (Badra *et al*., 2005; Heintze and Forjanic, 2005). Also, another important issue on wear processes is the brushing abrasion (Kawai *et al*., 1998). After a continuous brushing, the surface of the materials make them rougher and, consequently, prone to staining, plaque accumulations, and recurrent caries (Garcia *et al.*, 2004; Yap *et al*., 2005). In this manner, brushing abrasion and surface roughness analysis play an important role so that the material smoothness can be evaluated.

Moreover, as aforementioned, the remineralization of the demineralized enamel is also an important feature to be analyzed. The technology to detect and quantitative and qualitatively evaluate carious lesions in vitro has greatly evolved. Traditional methods of analysis such as transverse microradiography (Bergman and Engfeldt, 1954), Knoop microhardness (Sweeney, 1942), Vickers microhardness (Gustafson and Kling, 1948), polarized light microscopy (Carlström, 1964) and confocal laser scanning microscopy (Jones and Boyde, 1987) are effective methods.

With the addition of bioactive particles, the materials would be capable to penetrate into the enamel lesion in order to promote a higher hardness of the enamel lost strucuture. Thus, considering the good capability of penetration of the infiltrant materials, the capability of some bioactive particles to remineralize the demineralized enamel, and that there are no studies showing the addition of bioactive particles into an infiltrant so far, in our study, we added bioactive particles into an experimental infiltrant in order to evaluate the brushing wear resistance, the potential Knoop hardness depth analysis by micro-hardness, and the penetration capability of the experimental infiltrant materials and an available commercially material (ICON®) into the enamel initial lesion. The hypothesis tested were that: 1) the bioactive particles incorporated into the experimental materials would not affect the surface smoothness of the materials after brushing cycle; 2) all the materials would be able to penetrate into the enamel initial lesion; 3) the placement of experimental materials with bioactive particles on enamel initial lesion would increase the micro-hardness of mineral-depleted enamel over time in the presence of the bioactive particles.

2. MATERIALS AND METHODS

2.1. Experimental infiltrant preparation

The compositions of resin infiltrants are described in **Table 1**. The mixture of triethylenoglycol dimethacrylate (TEGDMA – 75 wt%) (Sigma-Aldrich Inc., St. Louis, MO, USA, Batch #01612M) and ethoxylated bisphenol A glycidyl dimethacrylate (BisEMA – 25 wt%) (Sigma-Aldrich Inc., St. Louis, MO, USA, Batch #03514HF) was used as an experimental control blend. Hydroxyapatite (Sigma-Aldrich Inc., St. Louis, MO, USA), amorphous calcium phosphate (Sigma-Aldrich Inc., St. Louis, MO, USA), bioactive glasses particles (BAG-Zn, BAG 45S5) and β-tricalcium phosphate modified calcium silicate cements (HCAT-β) bioactive particles were added in each control blend (10 wt%). The bioactive particles were added to the experimental infiltrant materials and agitated for 24 h, and also, the materials were slightly agitated before the application again. The photoinitiatior system selected was camphorquinone (CQ) (Sigma-Aldrich Inc., St. Louis, MO, USA, Batch #532604), and dimethyl aminoethyl methacrylate (DMAEMA) (Sigma-Aldrich, Inc., St. Louis, MO, USA, Batch #BCBF8391V) (proportion 1:2 by weight; 0.5% CQ/1% DMAEMA).

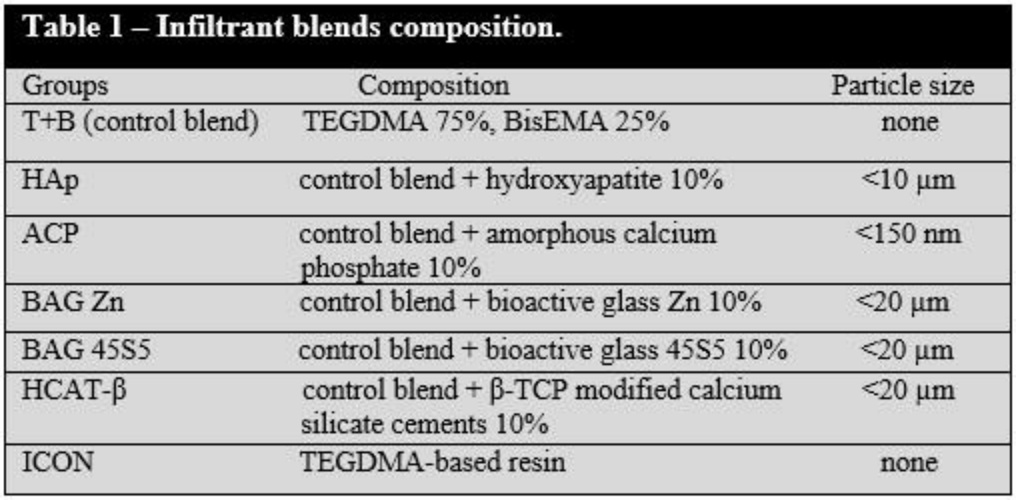

Table 1 – Infiltrant blends composition.

Groups	Composition	Particle size
T+B (control blend)	TEGDMA 75%, BisEMA 25%	none
HAp	control blend + hydroxyapatite 10%	<10 µm
ACP	control blend + amorphous calcium phosphate 10%	<150 nm
BAG Zn	control blend + bioactive glass Zn 10%	<20 µm
BAG 45S5	control blend + bioactive glass 45S5 10%	<20 µm
HCAT-β	control blend + β-TCP modified calcium silicate cements 10%	<20 µm
ICON	TEGDMA-based resin	none

% (wt%); TEGDMA: triethylene glycol dimethacrylate; BisEMA: ethoxylated bisphenol-A dimethacylate.

2.2. Brushing abrasion and surface roughness

Seventy discs specimens (5 mm diameter x 2 mm thickness) of infiltrant materials were made using a polydimethylsiloxane mould for brushing abrasion and surface roughness procedures (**Figure 1**). Specimens were light-cured for 40 s at 1000 mW/cm^2 using light emitting diode Ultralume 5 (Ultradent, South Jordan, Utah, USA). Afterwards, specimens were stored individually in distilled water for 24 hours at 37ºC. Surfaces were polished with silicon carbide abrasive papers (600#, 1200# and 2000#-grit) under water coolant. A final polishing was performed with diamond pastes (Buehler, Ltd., Lake Buff, IL, USA) with decreasing grit 3, 1 and 0,25 µm. Specimens were ultrasonically cleaned for 10 min after each polishing step.

Measurements were carried out with a surface profilometer using a Ra parameter (µm). In each surface, three sequential readings were performed, with a length of 1.25 mm, a cutoff of 0.25 mm and a speed of 0.1 mm/s. The Ra of each specimen was obtained from the arithmetic mean of its three Ra readings.

Tooth brushing abrasion was done using a mechanical tooth-brushing machine (Equilabor brushing machine; Equilabor, Piracicaba, SP, Brazil), modified from the standard model by

British Standard Institution, with capacity to 8 samples. Toothbrushes with compact head and soft nylon bristles (Sorriso Original, Colgate-Palmolive Ind. Com. Ltda, São Paulo, SP, Brazil) were adapted in the tooth brushing simulating machine (Equilabor). Slurry was prepared according to ISO specification #14569-1, mixing 2:1 of deionized water and dentifrice (Sorriso, Colgate-Palmolive Ind. Com. Ltda, São Paulo, SP, Brazil). Specimens were submitted to 30,000 brushing cycles under a frequency of 2 Hz, simulating a period of approximately three years of tooth brushing (Goldstein & Lerner, 1991). This apparatus provided linear tooth brushing movements across the specimens under a 200 g load and at a speed of 250 strokes/ min, with a double pass of the brush head over the surface. Toothbrushes were replaced after the completion of each brushing cycle. During brushing simulation, specimens were kept in distilled water.

Surface roughness measurements were conducted on the surface of infiltrant specimens in two moments: after the polishing procedure (baseline) and after the end of mechanical tooth brushing (**Figure 1**).

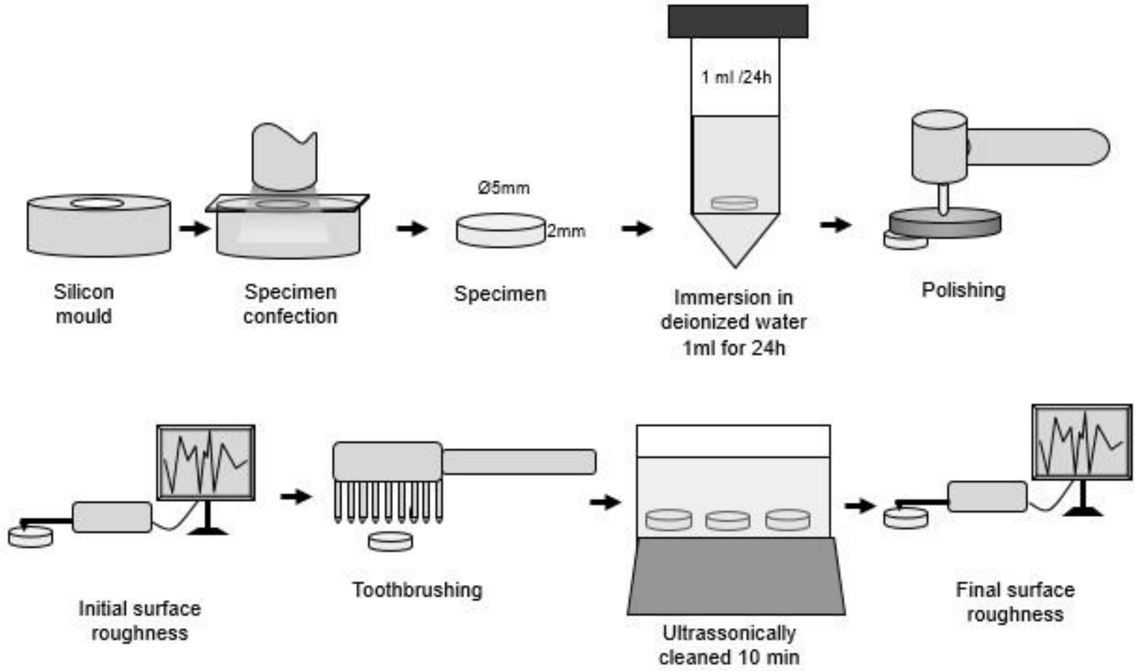

Figure 1. Schematic image showing brushing abrasion procedures

2.3. Artificial caries-like lesion formation

One hundred and fifteen sound third human molars were collected (thirty five for confocal analysis and eighty for micro-hardness). Approval was given by the Ethic Committee in Research of the Dental School of Piracicaba – UNICAMP, 006/2013 protocol. Teeth roots were removed and discarded. The sound surfaces were covered with two layers of acid-resistant nail varnish (Colorama®, São Paulo, Brazil), leaving an area of sound enamel on the vestibular surface (3 mm x 2mm) for micro-hardness analysis and on the occlusal surface (5 mm x 5 mm) for confocal microscopy. Each specimen was put individually into 50 mL (2.0 mL/mm^2 of exposed enamel) of 0.05 M acetate buffer solution, pH 5.0, at 50% hydroxyapatite saturation, for 10 h at 37ºC (Paes Leme *et al*., 2003).

2.4. Sample preparation

One hundred and fifteen (eighty for micro-hardness test and thirty five for confocal analysis) freshly extracted human molar teeth were used following the Ethics Committee in research of the Dental School of Piracicaba with protocol #006/2013. The teeth were submitted to the artificial-caries like lesion formation as aforementioned. For micro-hardness analysis, a carious group was set up as control (demineralized group). Caries-like lesions were etched with 37% phosphoric acid gel (H_3PO_4; Aldrich Chemical) for 60 s (Meyer-Lueckel *et al*., 2007), washed with water spray, and rinsed for 15 s. Infiltrants were applied using a microbrush, and left to penetrate for 60 s (Meyer-Lueckel *et al*., 2006). All infiltrants were light-cured for 60 s with 600 mW/cm^2 irradiance (Optilux VLC; Demetron, CT, USA).

2.5. Cycling demineralization/remineralization treatment

All the infiltrants were submitted to the cycling demineralization/remineralization treatment. The demineralizing solution (DS; Shinkai *et al*., 2001) used to mimic demineralizing oral fluids conditions has the following composition: acetic acid with 2.2 mmol/L $CaCl_2$, 2.2 mmol/L Na_3PO_4, 50 mmol/L acetate and 1 ppm fluoride and a pH 4.5 (adjusted by the addition of KOH). The remineralizing solution (RS; Shinkai *et al*., 2001) used to simulate remineralizing oral fluid conditions contained 1.5 mmol/L $CaCl_2$, 0.9 mmol/L Na_3PO_4 and

0.15 mmol/L KCl and had a pH equal to 7 (adjusted by the addition of KOH). The samples were alternately immersed in DS (1h) and RS (23 h) at 37° C for 30 d (Langhorst et al., 2009). Twenty mL of fresh DS or RS was used per specimen for each immersion, with continuous magnetic stirring provided. At every solution exchange, the samples and exposed (infiltrant) side of each specimen were rinsed with distilled water.

2.6. Micro-hardness analysis

Each infiltrant embedded in acrylic blocks were longitudinally sectioned through the center, polished and cross-sectional micro-hardness was measured using a Knoop micro-hardness tester (Model HMV-2, Shimadzu Corp., Tokyo, Japan). Three rows of 4 indentations each were made. The indentations were made at 50, 200, 350 and 500 µm from the outer to the inner enamel surface. The areas selected were 50 µm from the surface of the lesion to avoid indenting near to the surface (Amaechi and Higham, 2001).

2.7. Lesion infiltration and Confocal Laser Scanning Microscopy analysis (CLSM)

Caries-like lesions were etched with 37% phosphoric acid gel (H_3PO_4; Aldrich Chemical) for 60 s (Meyer-Lueckel *et al.*, 2007), washed with water spray, and rinsed for 15 s. Infiltrants were impregnated with 0.1% rhodamine B (Sigma-Aldrich, St. Louis, USA), applied onto the caries-like lesions using a microbrush, and left to penetrate for 60 s (Meyer-Lueckel *et al.*, 2006). All groups were light-cured for 60 s with >600 mW/cm^2 irradiance (Optilux VLC; Demetron, CT, USA). Next, tooth slabs with 2.0 mm thickness were obtained perpendicularly to the lesion surface, impregnated with the materials using a diamond saw (Isomet 1000, Buehler, Lake Bluff, IL, USA), and polished in a SiC papers series (1200# and 2400#-grit). To visualize the porous structure (not infiltrated lesions parts), specimens were immersed in a 50% ethanol solution of 100 µM sodium fluorescein (NaFl) (Sigma-Aldrich, St. Louis, USA) for 3 h and washed with deionized water for 10 s. Specimens were observed by CLSM (Leica SP2; Leica, Heidelberg, Germany) in dual-fluorescence mode and with a 63x oil objective lens. The excitation light had two wavelength maxima, at 488 and 568 nm. The emitted light was split by a 580-nm reflection short-pass filter and was passed through

525/50-nm band-pass filter for rodhamine B and a 590-nm long –pass filter for rodhamine B detection. Images with a lateral dimension of 1000 X 1000 μm^2 and a resolution of 1024 X 1024 pixels were recorded and analyzed by Leica SP2 CLSM software (Zeiss, Oberkochen, Germany). The evaluator was blind with regard to the group allocation of the teeth. CLSM was validated previously as a method to evaluate caries infiltration with excellent inter- and intra-examiner reproducibility in natural caries lesions (Paris *et al.*, 2009).

2.8. Statistical analysis

Data from surface roughness were submitted to two-way ANOVA (infiltrants and time) and Tukey's test (α=0.05). Also, micro-hardness analysis after a pH cycling was submitted to two-way ANOVA (infiltrants and treatments) and Tukey's test (α=0.05). Confocal analysis was qualitatively evaluated and the evaluator was blind with regard to the group allocation of the teeth.

3. RESULTS

Means and standard deviations of surface roughness before and after brushing abrasion are presented in **Table 2**. The outcomes showed that roughness of ACP before brushing was significantly lower than HAp, BAG Zn, BAG 45S5, HCAT-β and ICON®, and statistically similar to T+B. After brushing abrasion, BAG Zn, HCAT-β and ICON® were statistically similar among them, and showed the highest values comparing to the other groups. T+B, HAp and BAG Zn showed intermediate values, and were similar among them. ACP showed the lowest value when compared to all the other groups. Comparing the groups before and after brushing, T+B and HCAT-β showed significant statistically difference, and their roughness increased after brushing. Regarding to HAp, ACP, BAG Zn, BAG 45S5 and ICON®, there was no significant statistically difference before and after brushing. HAp showed the same values; ACP and BAG Zn showed decreased roughness after brushing; however, BAG 45S5 and ICON® showed increased roughness after brushing.

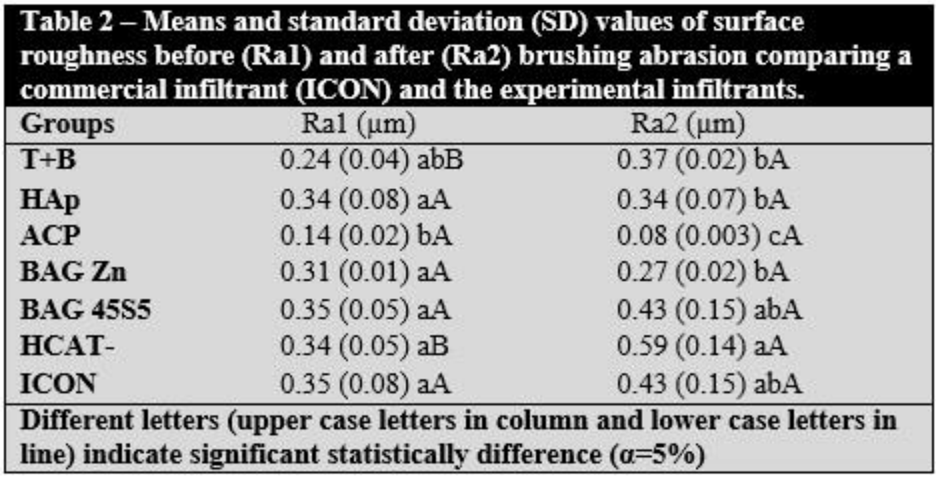

Table 2 – Means and standard deviation (SD) values of surface roughness before (Ra1) and after (Ra2) brushing abrasion comparing a commercial infiltrant (ICON) and the experimental infiltrants.

Groups	Ra1 (µm)	Ra2 (µm)
T+B	0.24 (0.04) abB	0.37 (0.02) bA
HAp	0.34 (0.08) aA	0.34 (0.07) bA
ACP	0.14 (0.02) bA	0.08 (0.003) cA
BAG Zn	0.31 (0.01) aA	0.27 (0.02) bA
BAG 45S5	0.35 (0.05) aA	0.43 (0.15) abA
HCAT-	0.34 (0.05) aB	0.59 (0.14) aA
ICON	0.35 (0.08) aA	0.43 (0.15) abA

Different letters (upper case letters in column and lower case letters in line) indicate significant statistically difference (α=5%)

Regarding to micro-hardness, there was no significant statistically difference among the evaluated depths ($p<0.05$). BAG 45S5, BAG Zn and HCAT-β did not show significant statistically difference among them ($p<0.05$). However, HCAT-β and BAG Zn was similar to ICON® and ACP as well. Moreover, BAG Zn, ACP and ICON® were statistically similar to T+B and HAp. Carious group showed the lowest value when compared to all the groups; except for T+B and HAp (**Table 3**).

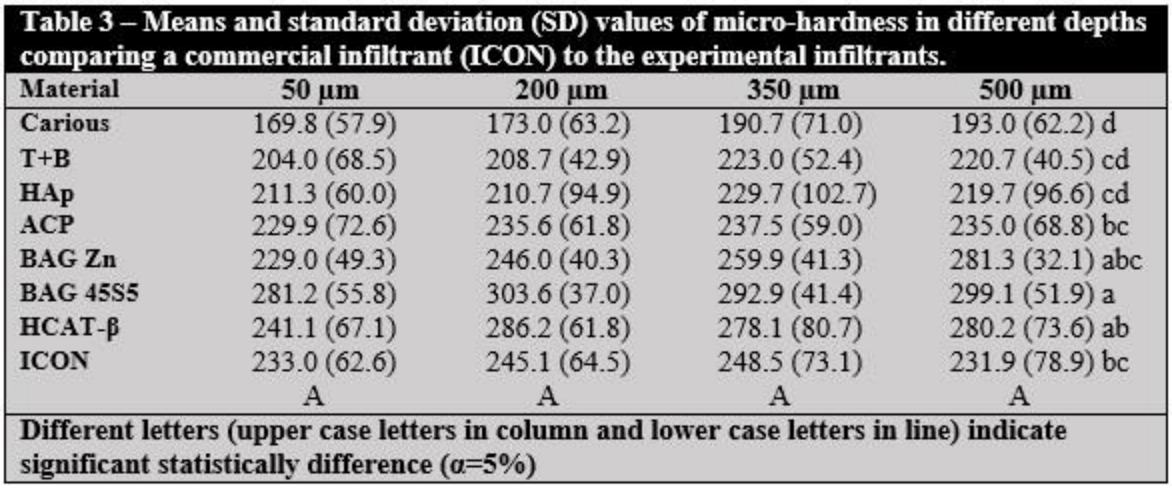

Table 3 – Means and standard deviation (SD) values of micro-hardness in different depths comparing a commercial infiltrant (ICON) to the experimental infiltrants.

Material	50 µm	200 µm	350 µm	500 µm
Carious	169.8 (57.9)	173.0 (63.2)	190.7 (71.0)	193.0 (62.2) d
T+B	204.0 (68.5)	208.7 (42.9)	223.0 (52.4)	220.7 (40.5) cd
HAp	211.3 (60.0)	210.7 (94.9)	229.7 (102.7)	219.7 (96.6) cd
ACP	229.9 (72.6)	235.6 (61.8)	237.5 (59.0)	235.0 (68.8) bc
BAG Zn	229.0 (49.3)	246.0 (40.3)	259.9 (41.3)	281.3 (32.1) abc
BAG 45S5	281.2 (55.8)	303.6 (37.0)	292.9 (41.4)	299.1 (51.9) a
HCAT-β	241.1 (67.1)	286.2 (61.8)	278.1 (80.7)	280.2 (73.6) ab
ICON	233.0 (62.6)	245.1 (64.5)	248.5 (73.1)	231.9 (78.9) bc
	A	A	A	A

Different letters (upper case letters in column and lower case letters in line) indicate significant statistically difference (α=5%)

Confocal microscopy was qualitatively analyzed. All the groups showed a good penetration capability into the whole extension of the lesion body, except for ACP group, which showed a decreased penetration of the material. Demineralized areas were evaluated as a translucent area using the reflection mode, and clear enamel prisms were shown. Demineralized areas were impregnated with 50% ethanol solution of 100 µM sodium fluorescein (NaFl), and was evaluated by fluorescence mode, indicating the green areas. Group HAp did not show the demineralized enamel impregnated as well as the other groups. Red areas show the infiltrants impregnated with 0.1% rhodamine B. ACP showed an irregular penetration along the lesion body, and a superficial barrier was created on the enamel. The overlapping of red and green areas were shown as the demineralized lesion, green labelled caries and red labelled infiltrants in an only image. Confocal micrographs are presented in **Figure 2.**

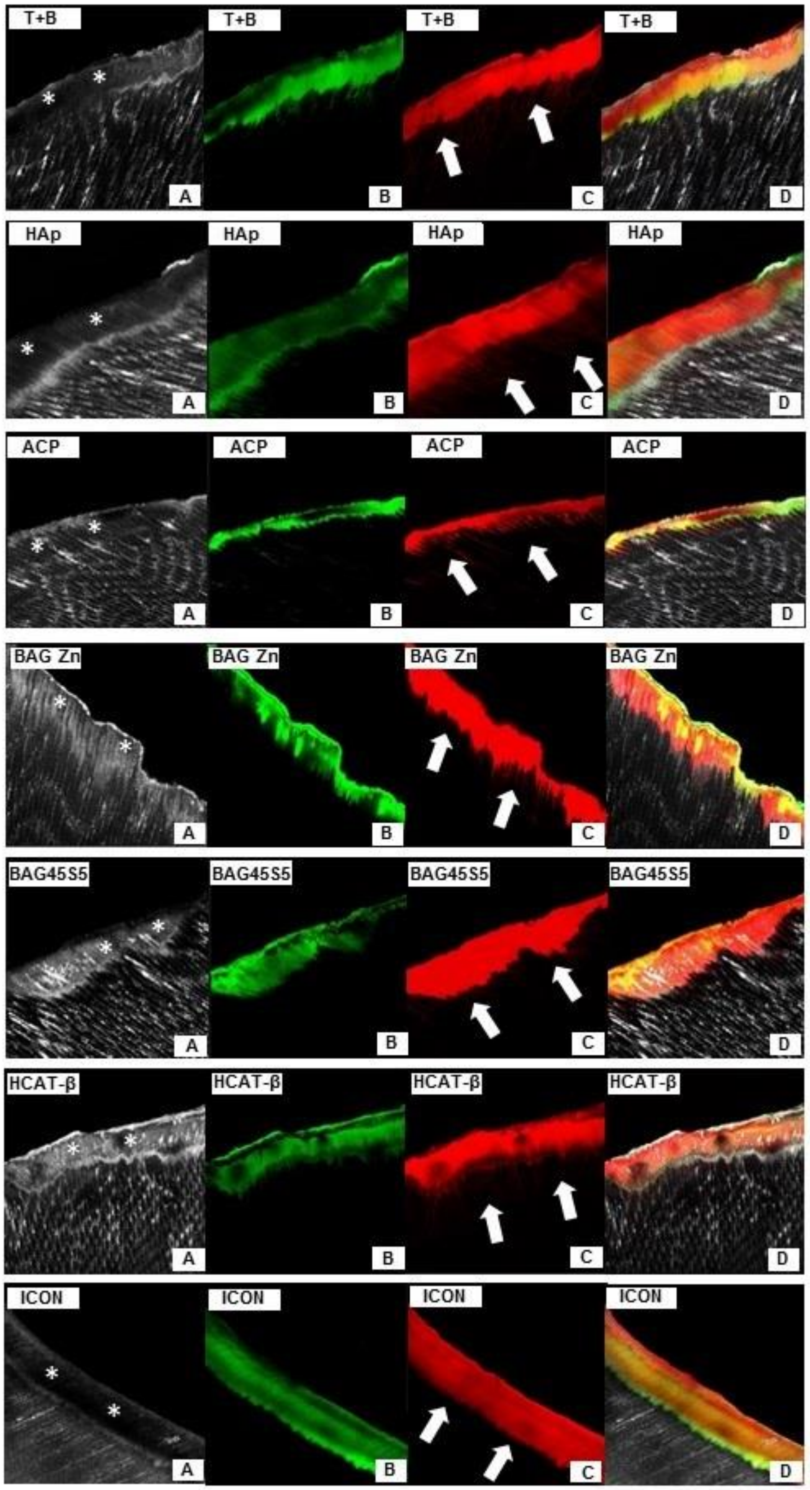
T+B
A
B
C
D
HAp
A
B
C
D
ACP
A
B
C
D
BAG Zn
A
B
C
D
BAG45S5
A
B
C
D
HCAT-β
A
B
C
D
ICON
A
B
C
D

Figure 2. Confocal micrographs showing the penetration of infiltrants. Note the demineralized area (asterisks in Figures A). The green areas show the demineralized areas impregnated with sodium fluorescein (Figures B). Sequentially, red areas show the rodhamine B impregnated infiltrant into the lesion body, indicating a good penetration along the caries extension (arrows), for all groups except for ACP, which shows an irregular penetration of the infiltrant. The Figure D show the overlapping of the green area and red area, indicating the infiltration of the rodhamine B impregnated materials into the lesion body labeled with sodium fluorescein.

4. DISCUSSION

This present study investigated the surface roughness, the potential Knoop hardness depth analysis by micro-hardness after a pH cycling, and the penetration capability of experimental infiltrants (with or without the addition of bioactive particles) and an available commercially infiltrant (ICON®). Statistical analysis showed that the bioactive particles incorporated to the experimental infiltrants affected the surface smoothness of the materials after brushing abrasion, except for ACP group. In this manner, the first hypothesis tested could be rejected. Also, the Knoop hardness depth analysis by micro-hardness showed an increase of hardness for all groups when compared to a carious group, however, infiltrants containing BAG Zn, BAG 45S5 and HCAT-β presented the highest hardness values. Thus, the second hypothesis tested could be accepted. Regarding to the confocal analysis, all the materials showed a good penetration into the lesion body, except ACP, which showed irregular infiltration, so the third hypothesis could be partially accepted.

Surface roughness and wear tests after simulated brushing abrasion have been indicated to assess the mechanical features of restorative materials (Cilli *et al.*, 2009; Cunha *et al.*, 2003; Garcia *et al.*, 2004; Prakki *et al.*, 2008; Wang *et al.*, 2004). Simulated brushing can intentionally provoke a stress in the organic matrix, fillers and their interfaces, and adhere to an assessment of their resistance properties (Mondelli *et al.*, 2009). Surface roughness exceeding a threshold Ra value of 0.2 µm is claimed to affect plaque accumulation and staining *in vitro* (Bollen *et al.*, 1997). Our results showed that ACP group presented values lower than 0.2 µm (0.08 µm) after brushing, indicating adequate surface roughness so that there is no bacterial retention, and consequently, plaque accumulation. We suppose that it may have been occurred due to its particle size, as ACP is the only nanosized particle group. Although a previous study (Oliveira *et al*, 2011) have investigated resin composites, and not infiltrants, by analogy, it is possible to compare their results with our findings. Oliveira *et al.*, 2011 showed that the nanofilled resins (Filtek Z350 and Concept Advanced) presented the smoothest surfaces. This was somehow expected as they are categorized as nanofilled resins. Nanofilled materials have the ability to provide more volume of filler in homogeneous distribution, which enables it to protect organic matrix wear (Cilli *et al*, 2009; Turssi *et al*, 2001). Another earlier study showed that the incorporation of nanofillers in restorative materials improves the abrasive resistance because it promotes a higher filler loading with smaller particle size and provides a reduction in the interparticle spacing, which effectively protects the softer matrix, reduces the incidence of filler exfoliation, and enhances the overall resistance of the material to abrasion (Söderholm & Richards, 1998).

Regarding to Knoop hardness depth analysis by micro-hardness test, all the experimental infiltrants (with or without the addition of bioactive particles), and also, ICON® showed an increased hardness value when compared to the carious surface. Paris *et al.* (2013) showed that caries infiltration significantly increase micro-hardness and reduce mineral loss after a demineralization challenge when compared with untreated lesions. Also, repeated resin application improves lesion micro-hardness and seems to have benefical effects on demineralization resistance, too. Taher *et al.* (2012) compared a fissure sealant with ICON® with regard to their surface hardness. The authors also showed that enamel surface treated with ICON® was approximately the same as that of sound enamel. Also, another study showed that the micro-hardness of initial enamel carious lesions increased significantly with the resin-infiltration technique and the final micro-hardness after a new acid challenge was similar when comparing the specimens infiltrated with resin and treated with 0.05% daily fluoride solution (Torres *et al.*, 2012). These findings could be explained because the infiltration technique aims to create a diffusion barrier inside the lesion, by replacing lost minerals with resin infiltrants (Paris *et al.*, 2007b).

According to the CLSM analysis, the addition of bioactive particles into the experimental infiltrants did not significantly affect the penetrability of the materials into the lesion body, except for ACP group. This fact could be explained due to its more viscous feature after addition of nanosized particles into the blend (T+B) when compared to the mixture of the other groups. The experimental materials which presented 75 wt% TEGDMA in its composition and ICON® (TEGDMA-based resin) showed a good penetration into the lesion body and along the lesion. Its low molecular weight (286 g/mol^{-1}) and low viscosity (η=0.05 Pa·s) reduce the viscosity of the material (Atai and Watts, 2006; Floyd and Dickens, 2006), which may promote the better penetration of the materials into the lesion body. We suppose that the bioactive particles (with μm sized particles) have been precipitated on the enamel and stuck them due to the polymerization. Further studies are needed in order to evaluate the remineralization capability of the experimental materials incorporated with bioactive particles on the demineralized enamel.

5. CONCLUSIONS

Overall, the results of this study showed that ACP showed the best results for surface roughness before and after brushing cycle. All the infiltrants tested showed increased micro-hardness after pH cycling. Also, infiltrants showed a good penetration into the enamel lesion body for all materials, except for ACP, according to the confocal analysis.

6. ACKNOWLEDGEMENTS

The authors wish to thank Capes-Brazil for the research grant 3352-13-7, and DMG from Brazil for providing ICON® kits. We are very grateful to Prof. Salvatore Sauro for the assistance with Confocal Microscopy analysis.

7. REFERENCES

1. Ahovu-Saloranta A, Hiiri A, Nordblad A, Makela M, & Worthington HV. Pit and fissure sealants for preventing dental decay in the permanent teeth of children and adolescents. Cochrane Database of Systematic Reviews, 2008: (4) CD001830.
2. Amaechi BT, Highman SM. In vitro remineralisation of eroded enamel lesion by saliva. J Dent 2001;29:371-376.
3. Atai M, Watts DC. A new kinetic model for the photopolymerization shrinkage-strain of dental composites and resin-monomers. Dent Mater 2006;22:785-791.
4. Badra VV, Faraoni JJ, Ramos RP, Palma-Dibb RG. Influence of different beverages on the microhardness and surface roughness of resin composites. Oper Dent 2005;30:213-219.
5. Banerjee A, Thompson ID, Watson TF. Minimally invasive caries removal using bioactive glass air-abrasion. J Dent 2011;39:2-7.
6. Bergman G, Engfeldt B. Studies on mineralized dental tissues. II: Microradiography as a method for studying dental tissues and its application to the study of caries. Acta Odontol Scand 1954; 12(2):99-132.
7. Bollen CM, Lambrechts P, Quirynen M. Comparison of surface roughness of oral hard materials to the threshold surface roughness for bacterial plaque retention: A review of the literature. Dent Mater 1997;13:258-269.
8. Carlström D. Polarization microscopy of dental enamel with reference to incipient carious lesions. In: Staple OH, editor. Advances in oral biology New York: Academic Press; 1964, p. 255-96.
9. Cao Y, Mei ML, Xu JG, Lo ECM, Li QL, Chu CH. Biomimetic mineralization of phosphorylated dentine by CPP-ACP. J Dent 2013;41:818-25.
10. Cilli R, Mattos MC, Honorio HM, Rios D, Araujo P, Prakki A. The role of surface sealants in the roughness of composites after a simulated toothbrushing test. J Dent 2009;37:970-7.

11. Cochrane NJ, Cai F, Huq NL, Burrow MF, Reynolds EC. New approaches to enhanced remineralization of tooth enamel. J Dent Res 2010;89(11):1187-97.
12. Cunha LG, Alonso RCB, Santos PH, Sinhoreti MAC. Comparative study of the surface roughness of Ormocer-based and conventional composites. J Appl Oral Sci 2003;11:348-53.
13. de Fucio SB, Puppin-Rontani RM, de Carvalho FG, Mattos-Graner R de O, Correr-Sobrinho L, Garcia-Godoy F. Analyses of biofilms accumulated on dental restorative materials. Am J Dent 2009;22:131-136.
14. Fan Y, Nelson JR, Alvarez JR, Hagan J, Berrier A, Xu X. Amelogenin-assisted *ex vivo* remineralization of human enamel: effects of supersaturation degree and fluoride concentration. Acta Biomater 2011;7:2293-302.
15. Featherstone JDB. Remineralization, the natural caries repair process – the need for new approaches. Adv Dent Res 2009;21:4-7.
16. Floyd CJ, Dickens SH. Network structure of BisGMA and UDMA-based resin systems. Dent Mater 2006; 22(12):1143-9.
17. Garcia FC, Wang L, D'Alpino PH, Souza JB, Araújo PA, Mondelli RF. Evaluation of the roughness and mass loss of the flowable composites after simulated toothbrushing abrasion. Braz Oral Res 2004;18:156-61.
18. Goldstein GR, Lerner T. The effect of toothbrushing on a hybrid composite resin. J Prosthet Dent, 1991; 66 (4): 498-500.
19. Gorelick L, Geiger AM, Gwinnett AJ. Incidence of white spot formation after bonding and banding. Am J Orthod 1982; 81:93-8.
20. Gustafson G, Kling O. Microhardness measurements in the human dental enamel. Odontol Tidskrift 1948;36:24-44.
21. Heintze SD, Forjanic M. Surface roughness of different dental materials before and after simulated toothbrushing *in vitro*. Oper Dent 2005;30:617-626.
22. Jones SJ, Boyde A. Scanning microscope observations on dental caries. Scanning Microsc 1987;1(4):1991-2002.
23. Kawai K, Iwuami Y, Ebisu S. Effect of resin monomer composition on toothbrush wear resistance. J Oral Rehabil 1998;25:264-268.

24. Langhorst SE, O'Donnell JNR, Skrtic D. *In vitro* remineralization of enamel by polymeric amorphous calcium phosphate composite: quantitative micro-radiographic study. Dent Mater 2009; 25(7): 884-891.
25. Lausch J, Paris S, Selje T, Dörfer CE, Meyer-Lueckel H. Resin infiltration of fissure caries with various techniques of pretreatment in vitro. Caries Res 2015; 49:50-55.
26. Lynch RJM, Smith SR. Remineralization agents: New and effective or just marketing hype? Adv Dent Res 2012;24:63.
27. Marinho VCC, Worthington HV, Walsh T, Clarkson JE. Fluoride varnishes for preventing dental caries in children and adolescents. Cochrane database of Syst Rev 2013:7.
28. Mejare I, Lingstrom P, Petersson LG, Holm AK, Twetman S, Kallestal C, Nordenram G, Lagerlof F, Soder B, Norlund A, Axelsson S, Dahlgren H. Caries-preventive effect of fissure sealants: A systematic review. Acta Odontol Scand, 2003; 61(6):321-330.
29. Meyer-Lueckel H, Paris S, Muller J, Cöefen H, Kielbassa AM. Influence of application time on the penetration of different dental adhesives and a fissure ealant into artificial subsurface lesions in bovine enamel. Dent Mater 2006;22:22-8.
30. Mondelli RFL, Azevedo JF, Francisconi PA, Ishikirama SK, Mondelli J. Wear and surface roughness of bovine enamel submitted to bleaching. Eur J Esthet Dent 2009;4:396-403.
31. Oliveira GU, Mondelli RFL, Charantola Rodrigues M, Franco EB, Ishikiriama SK, Wang L. Impact of filler size and distribution on roughness and wear of composite resin after simulated toothbrushing. J Appl Oral Sci 2011;510-516.
32. Paes Leme AF, Tabchoury CP, Zero DT, Cury JA. Effect of fluoridated dentifrice and acidulated phosphate fluoride application on early artificial caries lesions. Am J Dent 2003;16:91-5.
33. Paris S, Bitter K, Renz H, Hopfenmuller W, Meyer-Lueckel H. Validation of two dual fluorescence techniques for confocal microscopic visualization of resin penetration into enamel caries lesions. Microsc Res Tech 2009;72:489-94.

34. Paris S, Hopfenmuller W, Meyer-Lueckel H. Resin infiltration of caries lesions: an efficacy randomized trial. J Dent Res 2010;89:823-6.
35. Paris S, Meyer-Lueckel AM, Kielbassa AM. Resin infiltration of natural caries lesions. J Dent Res 2007;86(7):662-666.
36. Paris S, Meyer-Lueckel H. Inhibition of caries progression by resin infiltration *in situ*. Caries Res 2010;(44):47-54.
37. Paris S, Meyer-Lueckel H. Masking of labial enamel white spot lesions by resin infiltration: a clinical report. Quintessence Int 2009;40:713-18.
38. Paris S, Schwendicke F, Seddig S, Müller W,-D, Dörfer C, Meyer-Lueckel H. Micro-hardness and mineral loss of enamel lesion after infiltration with various resins: Influence of infiltrant composition and application frequency *in vitro*. J Dent 2013;41:543-548.
39. Phark JH, Duarte Jr. S, Meyer-Lueckel H, Paris S. Caries infiltration with resins: a novel treatment option for interproximal caries. Compend Contin Educ Dent 2009;30:13-7.
40. Prakki A, Cilli R, Mondelli RF, Kalachandra S. *In vitro* wear, surface roughness and hardness of propanal-containing and diacetyl-containing novel composites and copolymers based on bisGMA analogs. Dent Mater 2008;24:410-7.
41. Rao A, Malhotra N. The role of remineralization agents in dentistry: a review. Compend Contin Educ Dent 2011;32:26-36.
42. Reynolds EC, Cai F, Shen P, Walker GD, Reynolds C, Yuan Y. Remineralization of enamel subsurface lesions by chewing gum with added calcium. J Dent 2009;37:763-768.
43. Reynolds EC. Calcium phosphate-based remineralization systems: scientific evidence? Aust Dent J 2008;53:268-273.
44. Shinkai RS, Cury AA, Cury JA. In vitro evaluation of secondary caries development in enamel and root dentin around luted metallic restoration. Oper Dent 2001;26(1):52-9.
45. Silverstone LM. The structure of carious enamel, including the early lesion. Oral Sci Rev 1973;3:100-160.

46. Söderholm KJ & Richards ND. Wear resistance of composite: a solved problem? Gen Dent 1998;46(3):256-263.
47. Steinberg S. A paradigm shift in the treatment of caries. Gen Dent, 2002: 50(4):333-338.
48. Sweeney WT. The Knoop indentation hardness instrument as a tool in dental research. J Dent Res 1942; 21(3):303Taher NM, Alkhamis HA, Dowadi SM. The influence of resin infiltration system on enamel microhardness and surface roughness: an in vitro study. Saudi Dent J, 2012:24(2):79-84.
49. Taher NM, Alkhamis HA, Dowaidi SM. The influence of resin infiltration system on enamel microhardness and surface roughness: An in vitro study. Saudi Dent J 2012; 24(2):79-84.
50. Torres CRG, Rosa PCF, Ferreira NS, Borges AB. Effect of carious infiltration technique and fluoride therapy on microhardness of enamel carious lesions. Oper Dent 2012, 37(4):363-369.
51. Tschoppe P, Meyer-Lueckel H. Effects of regular and highly fluoridated toothpastes in combination with saliva substitutes on artificial enamel caries lesions differing in mineral content. Arch Oral Biol 2012;57:931-9.
52. Tufekci E, Dixon JS, Gunsolley JC, Lindauer SJ. Prevalence of white spot lesions during orthodontic treatment with fixed appliances. Angle Orthod 2011;81:206-10.
53. Turssi CP, Magalhaes CS, Serra MC, Rodrigues Júnior AL. Surface roughness assessment of resin-based materials during brushing preceded by pH cycling simulations. Oper Dent 2001;26:576-84.
54. Wang L, Garcia FC, Amarante de Araújo P, Franco EB, Mondelli RF. Wear resistance of packable resin composites after simulated toothbrushing test. J Esthet Restor Dent 2004;16:303-15.
55. Yap AU, Wu SS, Chelvan S, Tan ES. Effect of hygiene maintenance procedures on surface roughness of composite restoratives. Oper Dent 2005;30:99-104.
56. Zhou YZ, Cao Y, Liu W, Chu CH, Li QL. Polydopamine-induced tooth remineralization. ACS Appl Mater Interfaces 2012;4:6901-10.

CONSIDERAÇÕES GERAIS

De acordo com o Capítulo 1, de maneira geral, os infiltrantes experimentais (com ou sem adição de partículas bioativas) melhoraram as propriedades químicas e mecânicas dos materiais quando comparadas com um infiltrante disponível comercialmente (ICON®), exceto para a densidade de ligação cruzada, no qual o ICON® apresentou maior densidade de ligação cruzada. Um alto grau de conversão da matriz orgânica está frequentemente relacionado a propriedades mecânicas superiores nos compósitos restauradores, diminuindo o risco de fratura e desgaste (Ferracane e Greener, 1986; Bouschlicher *et al.,* 2004). Para o grau de conversão (GC), os materiais experimentais mostraram maior GC quando comparados ao ICON®. De acordo com a resistência a flexão (RF) e *E*-Modulus, os materiais experimentais com adição de partículas remineralizantes não mostraram diferença significativa entre eles (Tabela 2). Estes maiores valores para GC, RF e *E*-Modulus dos materiais experimentais com adição de partículas podem ser explicados devido a própria incorporação dessas partículas nos materiais experimentais. De acordo com um estudo anterior (Belli *et al*., 2014), melhora no grau de conversão ocorreu após a adição de partículas. A função ativa de partículas durante a polimerização é suportada pela aceleração da reação mostrada durante a medida de viscosidade. As curvas de viscosidade durante a polimerização mostraram que a rede polimérica alcança níveis maiores de rigidez anteriores para adesivos particulados. Particularmente, Park *et al*. (1998) estudou compósitos com adição de ACP em um trabalho anterior. Os resultados mostraram que compósitos com adição de ACP têm propriedades mecânicas que são adequadas para aplicação como materiais de base e possivelmente como selantes também. Embora não tenha sido estudado em um material infiltrante, mas tenha mostrado resultados promissores para selantes, é possível fazer uma analogia com nossos resultados, uma vez que nosso estudo mostrou propriedades adequadas para infiltrantes a base de ACP. Também, em uma analogia com nosso estudo, um estudou anterior mostrou que a adição de partículas de HAp de tamanho aproximado de 10 µm de diâmetro a um cimento de ionômero de vidro convencional (CIV) indicou que a HAp age como adsorvente e agente iônico permutável, bem como um reforço, resultando em propriedades mecânicas e químicas melhores de CIV (Arita *et al.*, 2011).

Os menores valores de dureza inicial (KH1) e de resistência coesiva à tração foram encontrados para o grupo do ICON®; entretanto, o ICON® apresentou maior quantidade de ligação cruzada (Tabela 2, Capítulo 1). Uma justificativa plausível para estes resultados seria uma maior concentração de apenas TEGDMA no material. Um estudo anterior (Gonçalves *et al.,* 2010) mostrou, em termos gerais, maior grau de conversão quando o TEGDMA foi misturado com BisGMA e UDMA, o que pode ser explicado pela diminuição logarítmica na viscosidade dada pelo diluente de baixo peso molecular e altamente flexível. Entretanto, conforme a concentração de TEGDMA aumenta para mais de 70 mol%, há tendência a diminuição da conversão, provavelmente devido a maior ciclização a um conteúdo com maior quantidade de TEGDMA (Sideridou *et al.*, 2002; Lovell *et al.*, 1999a; Dickens *et al.*, 2003).

A mistura do material experimental TEGDMA + BisEMA (T+B) e a adição de partículas bioativas neste material experimental apresentaram valores adequados a propriedades mecânicas. Com relação a dureza inicial, os grupos com a presença de biovidro com adição de Zn (BAG Zn), hidroxiapatita (HAp), fosfato de cálcio amorfo (ACP) e cimento de silicato de cálcio modificado por β-tricálcio fosfato (HCAT-β) não apresentam diferença estatisticamente significante entre eles (Tabela 2, Capítulo 1). Entretanto, partículas de vidro BAG 45S5 não foram similares ao BAG Zn e apresentaram valor relativamente menor. De acordo com a resistência coesiva à tração, não houve diferença estatisticamente significante entre os grupos T+B, HAp, FCA, BAG Zn, BAG 45S5 e HCAT-β) (Tabela 2, Capítulo 1).

Um estudo prévio mostrou que a concentrações de TEGDMA maiores que 40 mol%, a menor viscosidade inicial e a maior tendência a ciclização durante a polimerização prolongam a quantidade de formação de rede necessária para alcançar a mobilidade que permite a autoaceleração. A ciclização contribui para a conversão, mas não para o desenvolvimento de rede geral e leva à heterogeneidade (Lovell *et al.*, 1999b; Poshusta *et al.*, 2002). Estruturas cíclicas fornecem uma media maior de mobilidade, tanto quanto aumenta a mobilidade de grupos pendentes e de ligação cruzada, com um efeito análogo daquelas plastificadores (Lovell *et al.*, 1999b). Pfeifer *et al.* (2011) também mostrou que maiores conteúdos de TEGDMA na porçao gel, tanto quanto maior conversão limitante, resulta em menor perda de volume livre após a extração (mesmo no caso de misturas ricas em TEGDMA, o volume livre geral poderia ser maior por causa da maior liberdade a rotação associada a estas moléculas), apontando a um aumento esperado da densidade de ligação cruzada.

A sorção de água e solubilidade levariam a uma variedade de processos químicos e físicos que podem resultar em efeitos deletérios na estrutura e função de polímeros dentais (Malacarne *et al.*, 2006). Um outro estudo mostrou que a adição de partículas aos adesivos resinosos poderia diminuir a degradação do material ao longo do tempo (Kalachandra, 1989). A longevidade das restaurações dentais está relacionada com a qualidade do polímero formado (Ferracane, 2006). De acordo com esses achados, este estudo mostrou que todos os materiais experimentais (com ou sem a adição de partículas bioativas) mostraram menor sorção de água quando comparado ao material comercial ICON®. Uma justificativa para estes resultados pode ser a composição dos materiais. Um estudo anterior mostrou que a sorção de água aumentou com a diminuição na conversão (Gajewski *et al.*, 2012). No capítulo 2, os resultados mostraram menor grau de conversão para o ICON®, o que explicaria a menor dureza Knoop, a menor resistência coesiva à tração e a maior sorção de água obtida pelo ICON®. A menor sorção de água do material experimental T+B pode ser explicada devido a presença do monômero BisEMA na sua composição. Isto está de acordo com um estudo prévio que mostrou a menor sorção de água para o BisEMA, devido a conversão relativamente alta e ao caráter hidrófobo da molécula (Lemon *et al.*, 2007). Com relação à solubilidade dos materiais estudados, ICON® e ACP apresentaram maiores valores de solubilidade comparado aos outros grupos. A alta solubilidade do ICON® pode ser explicada devido a alta quantidade de TEGDMA na sua composição. Um estudo mostrou que TEGDMA, devido a tendência à ciclização, apresentou maiores resultados de solubilidade, provavelmente devido aos oligômeros de menor peso molecular estarem presentes e prontos para lixiviar (Gajewski *et al.*, 2012). O comportamento de ACP pode estar relacionado ao tamanho da partícula utilizada neste estudo. ACP foi o único grupo com a adição de partículas nanométricas. A solubilidade tende a aumentar quando o tamanho da partícula diminui, devido ao fato da área da superfície das partículas por volume se tornar maior, o que facilita a reação de dissolução em meio aquoso. Este fato é determinante para a solubilidade do fosfato em fluido corpóreo simulado (Bertazzo *et al.*, 2004).

A rugosidade da superfície e testes de desgastes após escovação simulada tem sido indicados para avaliar as características mecânicas de materiais restauradores (Cilli *et al.*, 2009; Cunha *et al.,* 2003; Garcia *et al*., 2004; Prakki *et al*., 2008; Wang *et al*., 2004). No capítulo 2, em relação aos valores de rugosidade de superfície antes da escovação, os grupos HAp, FCA, BAG Zn, BAG 45S5 e HCAT-β não mostraram diferença estatisticamente significante entre eles. Entretanto, o grupo FCA apresentou o menor valor de rugosidade inicial. Após a escovação, o grupo ACP continuou apresentando o menor valor de rugosidade, indicando uma superfície mais uniforme (menos rugosa) (Tabela 2, Capítulo 2). Estes resultados podem ser explicados devido ao tamanho da partícula presente nas composições experimentais. ACP é o único grupo com partículas de tamanho nanométricos. Um estudo anterior (Oliveira *et al*., 2011) corrobora com os nossos resultados, o qual, embora o autor tenha analisado resinas compostas e não infiltrantes, as resinas nanoparticuladas (Filtek Z350 e Concept Advanced) apresentaram superfícies mais planas. Os materiais nanoparticulados tem a capacidade de fornecer mais volume de partículas na distribuição homogênea, o que capacita-o de proteger o desgaste da matriz orgânica (Cilli *et al*., 2009; Turssi *et al*., 2001). Além disso, outro estudo mostrou que a incorporação de nanopartículas em materiais restauradores melhora a resistência a abrasão pois promove maior carregamento de partículas com menores tamanhos e fornece redução no espaçamento interpartículas, o que aumenta a resistência geral dos materiais à abrasão (Söderholm & Richards, 1998).

Com relação aos resultados de micro-dureza do esmalte obtidos, todos os infiltrantes experimentais (com ou sem adição de partículas bioativas), e também, o ICON® mostraram aumento da dureza quando comparados à superfície cariada apenas. Entretanto, quando comparamos os infiltrantes entre si, BAG Zn, BAG 45S5 e HCAT-β mostraram maiores valores de dureza do que os outros infiltrantes. Outro estudo mostrou que a micro-dureza de lesões iniciais de cárie em esmalte aumentaram significativamente com a técnica de infiltração e a micro-dureza final após um novo desafio ácido foi similar quando comparando espécimes infiltrados com resina e tratados com 0.05% de solução de flúor diária (Torres *et al.*, 2012). Paris *et al.* (2013) mostrou que a infiltração da cárie aumenta significativamente a micro-dureza e reduz a perda mineral após a desmineralização quando comparado com as lesões não tratadas. Isto poderia ser explicado porque a técnica de infiltração ajuda a criar uma barreira de difusão dentro da lesão, substituindo os minerais perdidos com a resina (Paris *et al.*, 2007b).

Com relação a penetração dos infiltrantes avaliada pela Microscopia Confocal, de uma maneira geral, a adição de partículas bioativas nos infiltrantes experimentais não afetou significativamente a penetração destes materiais no corpo da lesão, exceto para ACP. Este fato poderia ser explicado devido a sua característica mais viscosa após a adição de nano partículas na mistura (T+B) quando comparado às misturas dos outros grupos. Os materiais experimentais a base de TEGDMA (75% em peso) e ICON® (material a base de TEGDMA) mostraram uma boa capacidade de penetração no corpo da lesão e ao longo desta lesão, não mostrando irregularidades. O baixo peso molecular (286 g/mol^{-1}) e baixa viscosidade (η=0.05 Pa·s) do monômero TEGDMA aumenta sua fluidez (Atai e Watts, 2006; Floyd e Dickens, 2006), o que pode promover a melhor penetração e uniformidade do material no corpo da lesão. Entretanto, a análise em Microscopia Confocal de Varredura a laser indicou uma boa capacidade de penetração e homogeneidade para todos materiais experimentais, mesmo após a adição de partículas. Nós supomos que as partículas bioativas (com tamanhos micrométricos) tenham sido precipitadas sobre o esmalte, fazendo com que a mistura de T+B tenha penetrado dentro da lesão.

CONCLUSÃO

Diante dos resultados obtidos neste estudo, pode ser concluído que:

1. A adição de partículas bioativas em um infiltrante experimental apresentou melhor desempenho com relação às propriedades químico-mecânicas, mostrando melhora nas propriedades quando comparadas ao infiltrante comercial (ICON®).

2. O infiltrante resinoso contendo fosfato de cálcio amorfo foi o que apresentou os melhores resultados para rugosidade de superfície antes e após a escovação.

3. Todos os infiltrantes mostraram aumento da micro-dureza do esmalte após a ciclagem de pH. Os materiais mostraram boa capacidade de penetração e uniformidade no corpo da lesão, exceto o infiltrante com adição de ACP.

REFERÊNCIAS*

1. Ana ID, Matsuy S, Ohta M, Ishikawa K. Effects of added bioactive glass on the setting and mechanical properties of resin-modified glass ionomer cement. Biomater 2003;24:3061-7.
2. Arita K, Yamamoto A, Shinonaga Y, Harada K, Abe Y, Nakagawa K, Sugiyama S. Hydroxyapatite particle characteristics influence the enhancement of the mechanical and chemical properties of conventional restorative glass ionomer cement. Dent Mater J 2011; 30(5): 672-683.
3. Asmussen E, and Peutzfeldt A. A influence of pulse-delay curing on softening of polymer structures. J Dent Res 2001; 80:1570-1573.
4. Atai M, Watts DC. A new kinetic model for the photopolymerization shrinkage-strain of dental composites and resin-monomers. Dent Mater 2006;22:785-791.
5. Banerjee A, Hajatdoost-Sani M, FarrellS, Thompson I. A clinical evaluation and comparison of bioactive glass and sodium bicarbonate air-polishing powders. J Dent 2010;38:475-9.
6. Banerjee A, Thompson ID, Watson TF. Minimally invasive caries removal using bioactive glass air-abrasion. J Dent 2011;39:2-7.
7. Belli R, Kreppel S, Petschelt A, Hornberger H, Boccaccini AR, Lohbauer U. Strengthening of dental adhesives via particle reinforcements. J Mech Behav Biomed Mater 2014;37:100-108.
8. Bergman G, Engfeldt B. Studies on mineralized dental tissues. II: Microradiography as a method for studying dental tissues and its application to the study of caries. Acta Odontol Scand 1954; 12(2):99-132.

---

* *De acordo com a norma da UNICAMP/FOP, baseado na norma do International Committee of Medical Journal Editors – Grupo de Vancouver. Abreviatura dos periódicos em conformidade com o Medline*

9. Bertazzo S, Bertran CA. Solubilidade de fosfatos de cálcio em fluído corpóreo simulado. Biocompatibilidade e propriedades da interface fosfato de cálcio/solução. UNICAMP 2004.
10. Bjarnason S, Finnbogason SY. Effect of different fluoride levels in dentifrice on the development of approximal caries. Caries Res 1991;25:207-212.
11. Bonilla ED, Yashar M, and Caputo AA. Fracture toughness of nine flowable resin composites. J Prosthet Dent 2003; 89:261-267.
12. Bouschlicher MR, Rueggeberg FA, Wilson BM. Correlation of bottom-to-top surface microhardness and conversion ratios for a variety of resin composite compositions. Oper Dent 2004;29(6):698-704.
13. Carlström D. Polarization microscopy of dental enamel with reference to incipient carious lesions. In: Staple OH, editor. Advances in oral biology New York: Academic Press; 1964, p. 255-96.
14. Cilli R, Mattos MC, Honorio HM, Rios D, Araujo P, Prakki A. The role of surface sealants in the roughness of composites after a simulated toothbrushing test. J Dent 2009;37:970-7.
15. Cunha LG, Alonso RCB, Santos PH, Sinhoreti MAC. Comparative study of the surface roughness of Ormocer-based and conventional composites. J Appl Oral Sci 2003;11:348-53.
16. Davidson CL, Hoekstra IS, Arends J. Microhardness of sound, decalcified and etched tooth enamel related to the calcium content. Caries Res 1974;8(2):135-44.
17. Dickens SH, Flaim GM, Takagi S. Mechanical properties and biochemical activity of remineralizing resin-based $CaPO_4$ cements. Dent Mater 2003;19:558-566.
18. Featherstone JD. Caries prevention and reversal based on the caries balance. Pediatr Dent 2006;28:128-32
19. Ferracane JL, Greener EH. The effect of resin formulation on the degree of conversion and mechanical properties of dental restorative resins. J Biomed Mater Res 1986;20:121-131.

20. Ferracane JL. Hygroscopic and hydrolytic effects in polymer networks. In: Proceedings of conference on scientific insights into dental ceramics and photopolymer networks, vol. 18. 2004. P. 118-28.
21. Ferracane JL. Hygroscopic and hydrolytic effects in dental polymer networks. Dent Mater 2006;22:211-22.
22. Floyd CJ, Dickens SH. Network structure of BisGMA- and UDMA-based resin systems. Dent Mater 2006;22(12):1143-9.
23. Gajewski VE, Pfeifer CS, Fróes-Salgado NR, Boaro LC, Braga RR. Monomers used in resin composites: degree of conversion, mechanical properties and water sorption/solubility. Braz Dent J 2012;23(5):508-514.
24. Garcia FC, Wang L, D'Alpino PH, Souza JB, Araújo PA, Mondelli RF. Evaluation of the roughness and mass loss of the flowable composites after simulated toothbrushing abrasion. Braz Oral Res 2004;18:156-61.
25. Gonçalves F, Pfeifer CS, Stansbury JW, Newman SM, Braga RR. Influence of matrix composition on polymerization stress development of experimental composites. Dent Mater 2010;26:697-703.
26. Guiraldo RD, Consani S, Consani RL, Berger SB, Mendes WB and Sinhoreti MA. Light energy transmission through composite influenced by materials shades. Bull. Tokyo Dent Coll 2009; 50: 183-190.
27. Gustafson G, Kling O. Microhardness measurements in the human dental enamel. Odontol Tidskrift 1948;36:24-44.
28. Hirayama S, Iwai H, Tanimoto Y. Mechanical evaluation of five flowable resin composites by the dinamic micro-indentation method. J Dent Biomechanics 2014; 5:1-8.
29. Ito A, Kawamura H, Otsuka M, Ikeuchi M, Ohgushi H, Ishikawa K, et al. Zinc-releasing calcium phosphate for stimulating bone formation. Mater Sci Eng 2002;22:21-25.
30. Ito A, Ojima K, Naito H, Ichinose N, Tateishi T. Preparation, solubility and cytocompatibility of zinc-releasing calcium phosphate ceramics. J Biomed Mater Res 2000;50(2):178-183.

31. Jones SJ, Boyde A. Scanning microscope observations on dental caries. Scanning Microsc 1987;1(4):1991-2002.
32. Kalachandra S. Influence of fillers on the water sorption of composites. Dent Mater 1989;5(4):283-8.
33. Kidd EAM, van Amerongen JP (2003). The role of operative treatment. In: Dental Caries: the disease and its clinical management. Kidd E, Fejerskov O, editors. Oxford: Blackwell Munksgaard, pp. 245-250.
34. Langhorst SE, O'Donnell JN, Skrtic D. *In vitro* remineralization of enamel by polymeric amorphous calcium phosphate composite: quantitative microradiographic study. Dent Mater 2009;25:884-891.
35. Lemon MT, Jones MS, Stansbury JW. Hydrogen bonding interactions in methacrylate monomers and polymers. J Biomed Mater Res Part A 2007;83A:734-746.
36. Lippert F, Lynch RJ. Comparison of Knoop and Vickers surface microhardness and transverse microradiography for the study of early caries lesion formation in human and bovine enamel. Arch Oral Biol 2014; 59(7):704-10.
37. Lovell LG, Newman SM, Bowman CN. The effects of light intensity, temperature, and comonomer composition on the polymerization behavior of dimethacrylate dental resins. J Dent Res 1999a;78(8):1469-76.
38. Lovell LG, Newman SM, Bowman CN. The effects of light intensity, temperature, and comonomer composition on the polymerization behavior of dimethacrylate dental resins. J Dent Res 1999b; 78(8): 1469-1476.
39. Lusvardi G, Malavasi G, Menabue L, Cannas M. Properties of zinc releasing surfaces for clinical applications. J Biomater Appl 2008;22:505-26.
40. Lynch RJM, Smith SR. Remineralization agents: new and effective or just marketing hype? Adv Dent Res 2012;24(2):63-67.
41. Malacarne J, Carvalho RM, de Goes MF, Svizero N, Pashley DH, Tay FR, Yiu CK, Carrilho MR. Water sorption/solubility of dental adhesive resins. Dent Mater 2006;22:973-980.

42. Meyer-Lueckel H, Paris S. Improved resin infiltration of natural caries lesions. J Dent Res 2008a;87:1112-1116.

43. Meyer-Lueckel H, Paries S. Progression of artificial enamel caries lesions after infiltration with experimental light curing resins. Caries Res 2008b;42:117-124.

44. Oliveira GU, Mondelli RFL, Charantola Rodrigues M, Franco EB, Ishikiriama SK, Wang L. Impact of filler size and distribution on roughness and wear of composite resin after simulated toothbrushing. J Appl Oral Sci 2011;510-516.

45. Paris S, Meyer-Lueckel H, Colfen H, Kielbassa AM. Resin infiltration of artificial enamel caries lesions with experimental light curing resins. Dent Mater J 2007a;26:582-588.

46. Paris S, Meyer-Lueckel AM, Kielbassa AM. Resin infiltration of natural caries lesions. J Dent Res 2007b;86(7):662-666.

47. Paris S, Schwendicke F, Seddig S, Müller W,-D, Dörfer C, Meyer-Lueckel H. Micro-hardness and mineral loss of enamel lesion after infiltration with various resins: Influence of infiltrant composition and application frequency *in vitro*. J Dent 2013;41:543-548.

48. Park MS, Eanes ED, Antonucci JM, Skrtic D. Mechanical properties of bioactive amorphous calcium phosphate/methacrylate composites. Dent Mater 1998;14:137-141.

49. Pfeifer CS, Shelton ZR, Braga RR, Windmoller D, Machado JC, Stansbury JW. Characterization of dimethacrylate polymeric networks: a study of the crosslinked structure formed by monomers used in dental composites. Eur Polym J 2011;47(2):162-70.

50. Poshusta AK, Bowman CN, Anseth KS. Application of a kinetic gelation simulation to the characterization of in situ cross-linking biomaterials. J Biomat Scie-Polymer Edition. 2002; 13(7): 797-815.

51. Prakki A, Cilli R, Mondelli RF, Kalachandra S. In vitro wear, surface roughness and hardness of propanal-containing and diacetyl-containing novel composites and copolymers based on BisGMA analogs. Dent Mater 2008;24:410-7.
52. Rao A, Malhotra N: The role of remineralizing agents in dentistry: A review. Compend Contin Educ Dent 2011;32:26-36.
53. Reynolds EC, Cai F, Cochrane NJ, Shen P, Walker GD, Morgan MV, et al. Fluoride and casein phosphopeptide-amorphous calcium phosphate. J Dent Res 2008b;87(4):344-8.
54. Reynolds EC, Cai F, Shen P, Walker GD, Reynolds C, Yuan Y. Remineralization of enamel subsurface lesions by chewing gum with added calcium. J Dent 2009;37:763-768.
55. Reynolds EC, Cai F, Shen P, Walker GD. Retention in plaque and remineralization of enamel lesions by various forms of calcium in a mouthrinse or sugar-free chewing gum. J Dent Res 2003;82(3):206-11.
56. Reynolds EC. Calcium phosphate-based remineralization systems: scientific evidence? Aust Dent J 2008a;53:268-273.
57. Santerre JP, Shajii L, Leung BW. Relation of dental composite formulations to their degradation and the release of hydrolyzed polymeric-resin-derived products. Crit Rev Oral Biol Med 2001; 12:136-51.
58. Sauro S, Osorio R, Watson TF, Toledano M. Therapeutic effects of novel resin bonding systems containing bioactive glasses on mineral-depleted areas within the bonded-dentine interface. J Mater Sci 2012;23:1521-32.
59. Schneider LF, Moraes RR, Cavalcante LM, Sinhoretti MA, Correr-Sobrinho L, Consani S. Cross-link density evaluation through softening test: Effect of ethanol concentration. Dent Mater 2008;24:199-203.
60. Sideridou I, Iserki V, Papanastasiou G. Effect of chemical structure on degree of conversion in light-cured dimethacrylate-based dental resins. Biomater 2002;23(8):1819-29.
61. Siverstone LM. Remineralization phenomena. J Caries Res 1977;11(suppl):59-84.

62. Skrtic D, Hailer AW, Takagaki S, Antonnucci JM, Eanes ED. Quantitative assessment of the efficacy of amorphous calcium phosphate/methacrylate composites in remineralizing caries-like lesions artificially produced in bovine enamel. J Dent Res 1996;75(9):1679-86.
63. Söderholm KJ & Richards ND. Wear resistance of composite: a solved problem? Gen Dent 1998;46(3):256-263.
64. Söderholm KJM, Mondragon E, Garcea I. Use of zinc phosphate cement as a luting agent for Denzir$^{\text{TM}}$ Copings: an in vitro study. BMC Oral Health 2003;3:1-8.
65. St-Georges AJ, Swift EJ Jr., Thompson JY, *et al*. Irradiance effects on the mechanical properties of universal hybrid and flowable hybrid resin composites. Dent Mater 2003; 19:406-13.
66. Sumino N, Tsubota K, Takamizawa T, *et al.* Comparison of the wear and flexural characteristics of flowable resin composites for posterior lesions. Acta Odontol Scand 2013; 71:820-27.
67. Sweeney WT. The Knoop indentation hardness instrument as a tool in dental research. J Dent Res 1942; 21(3):303
68. Ten Cate JM, Arends J. Remineralization of artificial enamel lesions in vitro: III. A study of the deposition mechanism. Caries Res 1980;14:351-358.
69. Ten Cate JM, Larsen MJ, Pearce EIF, Fejerskov O (2003). Chemical interactions between the tooth and oral fluids. In: Dental Caries. Fejerskov O, Kidd EAM, editors. Oxford: Blackwell Munksgaard, pp. 49-69.
70. Torres CRG, Rosa PCF, Ferreira NS, Borges AB. Effect of carious infiltration technique and fluoride therapy on microhardness of enamel carious lesions. Oper Dent 2012, 37(4):363-369.
71. Turssi CP, Magalhaes CS, Serra MC, Rodrigues Júnior AL. Surface roughness assessment of resin-based materials during brushing preceded by pH cycling simulations. Oper Dent 2001;26:576-84.
72. Vollenweider M, Brunner TJ, Knecht S, Grass RN, Zehnder M, Imfeld T, et al. Remineralization of human dentin using ultrafine bioactive glass particles. Acta Biomater 2007;3:936-43.

73. Walker GD, Cai F, Shen P, Adams GG, Reynolds C, Reynolds EC. Casein phosphopeptide-amorphous calcium phosphate incorporated into sugar confections inhibits the progression of enamel subsurface lesions *in situ.* Caries Res 2010;44:33-40.
74. Wang L, Garcia FC, Amarante de Araújo P, Franco EB, Mondelli RF. Wear resistance of packable resin composites after simulated toothbrushing test. J Esthet Restor Dent 2004;16:303-15.
75. Wang JY, Zhai WY, Ni Sy, Jiang Chang RLD. Characterization and in vitro bioactivity of zinc-containing bioactive glass and glass-ceramics. J Biomater Appl 2006;20:341-60.
76. Yamaguchi, M, Yamagushi R. Action of zinc on bone metabolism in rats increases in alkaline phosphatase activity and DNA content. Biochenl Pharmacol 1986;35:773-777.
77. Yap AU, Wu SS, Chelvan S, Tan ES. Effect of hygiene maintenenc procedures on surface roughness of composite restoratives. Oper Dent 2005; 30:99-104.

ANEXO 1

11/11/2014 Comitê de Ética em Pesquisa - Certificado

COMITÊ DE ÉTICA EM PESQUISA
FACULDADE DE ODONTOLOGIA DE PIRACICABA
UNIVERSIDADE ESTADUAL DE CAMPINAS

CERTIFICADO

O Comitê de Ética em Pesquisa da FOP-UNICAMP certifica que o projeto de pesquisa **"Avaliação das propriedades físico-químicas de infiltrantes experimentais com partículas bioativas"**, protocolo nº 006/2013, dos pesquisadores Ravana Angelini Sfalcin e Américo Bortolazzo Correr, satisfaz as exigências do Conselho Nacional de Saúde - Ministério da Saúde para as pesquisas em seres humanos e foi aprovado por este comitê em 12/03/2013.

The Ethics Committee in Research of the Piracicaba Dental School - University of Campinas, certify that the project **"Evaluation of the physical-chemical properties of experimental infiltrants incorporated with bioactive glass particles"**, register number 006/2013, of Ravana Angelini Sfalcin and Américo Bortolazzo Correr, comply with the recommendations of the National Health Council - Ministry of Health of Brazil for research in human subjects and therefore was approved by this committee on Mar 12, 2013.

Prof. Dr. Felippe Bevilacqua Prado
Secretário
CEP/FOP/UNICAMP

Lívia M A Tenuta
Profa. Dra. Lívia Maria Andaló Tenuta
Coordenadora
CEP/FOP/UNICAMP

Nota: O título do protocolo aparece como fornecido pelos pesquisadores, sem qualquer edição.
Notice: The title of the project appears as provided by the authors, without editing.

ANEXO 2

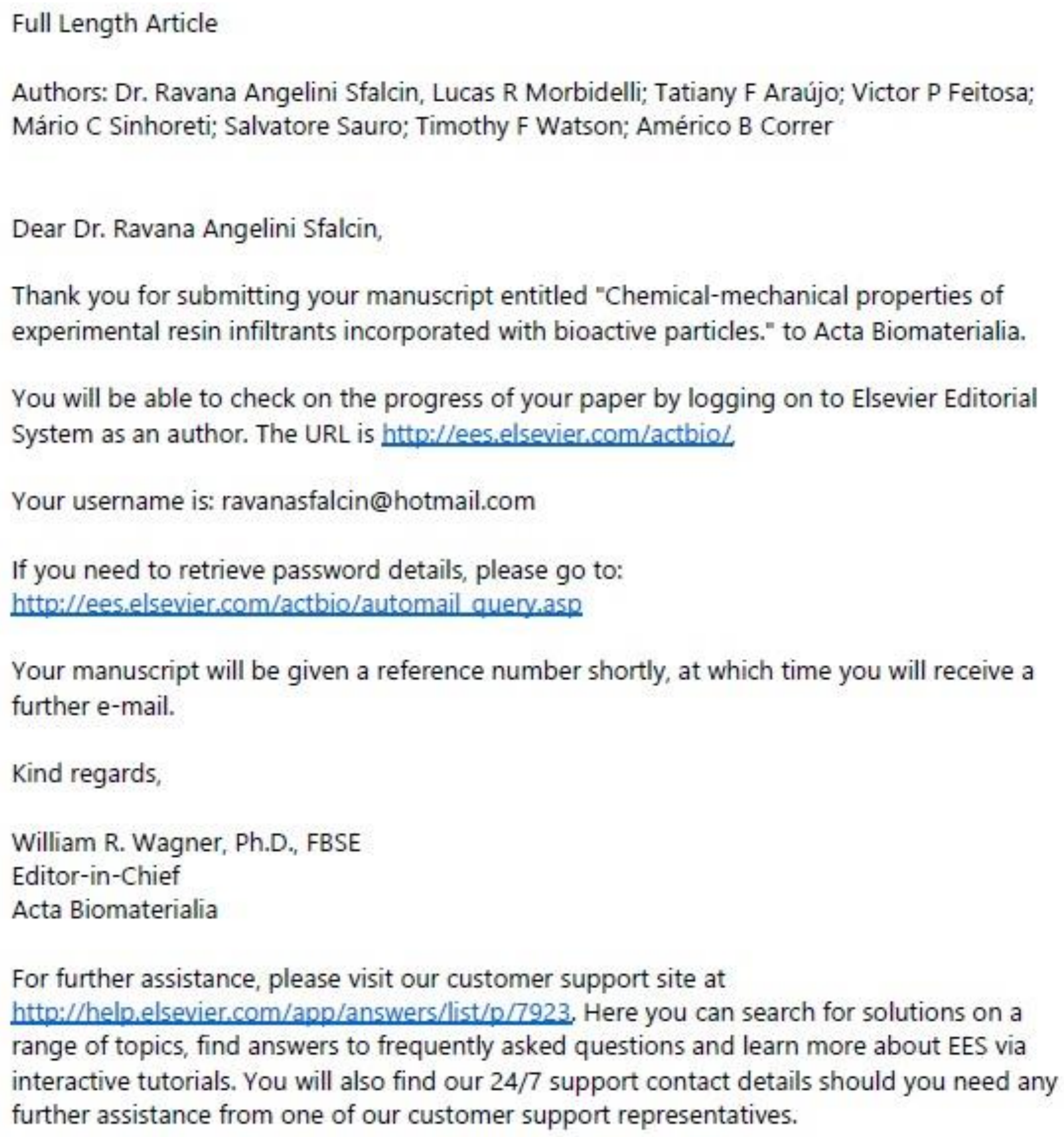

Full Length Article

Authors: Dr. Ravana Angelini Sfalcin, Lucas R Morbidelli; Tatiany F Araújo; Victor P Feitosa; Mário C Sinhoreti; Salvatore Sauro; Timothy F Watson; Américo B Correr

Dear Dr. Ravana Angelini Sfalcin,

Thank you for submitting your manuscript entitled "Chemical-mechanical properties of experimental resin infiltrants incorporated with bioactive particles." to Acta Biomaterialia.

You will be able to check on the progress of your paper by logging on to Elsevier Editorial System as an author. The URL is http://ees.elsevier.com/actbio/.

Your username is: ravanasfalcin@hotmail.com

If you need to retrieve password details, please go to:
http://ees.elsevier.com/actbio/automail_query.asp

Your manuscript will be given a reference number shortly, at which time you will receive a further e-mail.

Kind regards,

William R. Wagner, Ph.D., FBSE
Editor-in-Chief
Acta Biomaterialia

For further assistance, please visit our customer support site at http://help.elsevier.com/app/answers/list/p/7923. Here you can search for solutions on a range of topics, find answers to frequently asked questions and learn more about EES via interactive tutorials. You will also find our 24/7 support contact details should you need any further assistance from one of our customer support representatives.